7.3

Photochemical Processes

CHARLES KUTAL
University of Georgia, Athens, GA, USA
and
ARTHUR W. ADAMSON
University of Southern California, Los Angeles, CA, USA

7.3.1 INTRODUCTION

Inorganic photochemistry has progressed through several stages. We begin with a period of scattered observations extending to the early 1950s. Examples are Eder's reaction,[1] that is, the photoredox decomposition of $HgCl_2$ in the presence of oxalate ions, uranyl oxalate actinometry (ref. 2, for instance), and the classic blueprinting process in which the photoreduction of ferric citrate to Fe^{II} in the presence of ferricyanide ion leads to the formation of Turnbull's blue. Photoredox decompositions of Co^{III} complexes were studied by Vranek,[3] Schwarz and Tede,[4] and Linhard and Weigel.[5] There are also early observations of ligand photosubstitutions, as in the case of $PtCl_6^{2-}$.[6]

The foundations of the contemporary period were laid in the early 1960s with increasingly systematic studies of ammine complexes of Co^{III} and especially of Cr^{III}. In the latter case, these led to rules predictive as to which ligand would undergo photosubstitution in a mixed ligand complex.[7] Reference 8 reviews the photochemistry of this period.

The field matured rapidly during the 1970s, and in several directions. New phenomenology was discovered such as the photosensitization of Co^{III} ammine complexes,[9] and emission from Cr^{III} complexes in room temperature, fluid solution.[10] This last observation made emission quenching studies possible,[11] and from then on increasingly detailed and sophisticated investigations of excited state processes appear in the literature. Excited state electron transfer was observed,[12] with much stimulation of interest in the possibility of solar energy conversion through the solar splitting of water and like processes. The photochemistry of new families of Werner-type complexes was explored, such as those of Rh^{III}, Ir^{III} and Ru^{II}. Complexes with polypyridine-type ligands became of much interest. Systems involving coordinated sulfur and phosphorus were probed, as were new types of macrocyclic complexes, including those with biological relevance such as cobalamins and metalloporphyrins. Finally, the whole area of organometallic compounds received increasing attention.

Reviews that cover the field up to the middle 1970s are references 13–16. A useful contemporary series of review-type articles, intended for the more general reader, appeared in the October 1983 issue of the *Journal of Chemical Education*.

A qualitative profile of the current status of inorganic photochemistry is attempted in Table 1. Metals are grouped according to Periodic Table families, and ligands are differentiated according to whether they are of the traditional type (*e.g.* ammonia, saturated amines, pseudo-halogens), delocalized chelate/macrocyclic (*e.g.* 2,2′-bipyridine, porphyrin) or predominantly π-acid in character (*e.g.* carbonyl, alkene). In addition, the type of investigation performed is indicated. The best studied complexes are those of Cr^{III}, Co^{III} and the polypyridine complexes of Ru^{II}, while knowledge of the photobehavior of several elements is still rather primitive.

Table 1 Survey of Photochemistry and Photophysics of Coordination Compounds[a]

Metal	*Type of ligand*			*Type of study*			
	Ammine, cyano, etc.	*Delocalized chelate/macrocyclic*	*π-Acid*	*Photochemical*	*Photophysical*	*Mechanistic*	*Theoretical*
V	*	—	*	*	—	—	—
Nb	—	—	*	*	—	—	—
Ta	—	—	*	*	—	—	—
Cr	***	**	**	***	***	***	***
Mo	*	—	**	**	*	*	—
W	*	—	**	**	**	**	*
Mn	*	*	**	**	—	—	—
Tc	—	—	—	—	—	—	—
Re	—	—	*	*	*	—	—
Fe	**	**	**	**	*	*	*
Ru	*	***	**	***	***	***	***
Os	*	**	*	**	**	*	*
Co	***	**	**	***	*	***	***
Rh	**	*	**	**	**	**	**
Ir	*	*	*	*	*	*	*
Ni	*	*	*	*	—	—	—
Pd	*	*	*	*	—	—	—
Pt	**	*	—	**	**	**	**
Cu	**	**	—	**	—	*	*
Ag	***	—	—	***	—	*	—
Au	*	*	—	*	—	—	—
Zn	*	—	—	*	—	*	—
Cd	*	—	—	*	—	*	—
Hg	*	*	—	*	—	*	—
Actinides, lanthanides	**	*	—	**	*	*	*

[a] Asterisks denote extent of coverage: heavy (***), moderate (**) or light (*).

The plan of this article is as follows. In Section 7.3.2 we discuss the general physical chemistry of excited states and excited state processes. Section 7.3.3 surveys the characteristic reactivities of the various types of excited states found in *d* and *f* transition metal complexes (excluding organometallic compounds). Section 7.3.4 provides a brief account of some applications of transition metal photochemistry.

7.3.2 EXCITED STATES AND EXCITED STATE PROCESSES

7.3.2.1 Types of Excited States

Experimental information about excited states comes primarily from absorption spectra, and a fairly typical one for a transition metal ammine is shown in Figure 1, namely that of $[Cr(NCS)(NH_3)_5]^{2+}$ in aqueous solution. Transitions are characterized first of all by the energy, E, corresponding to the absorption band maximum. The Einstein relationship is given in equation (1), where h is Planck's constant, ν is the frequency at the band maximum, and $\bar{\nu}$ the corresponding wavenumber. Very commonly, band maxima positions are given in terms of their wavelength, λ. The second important quantity is the absorptivity, A (or optical density, D), defined by equation (2), where I_0 and I are the incident and emergent intensity of light in a beam passing through depth l of a solution of concentration C. The quantity ε is known as the extinction coefficient when expressed in M^{-1} cm^{-1} units (M denoting mol liter^{-1}); in SI units, it is called the molar absorptivity. Equation (2) is known as the Beer-Lambert Law.

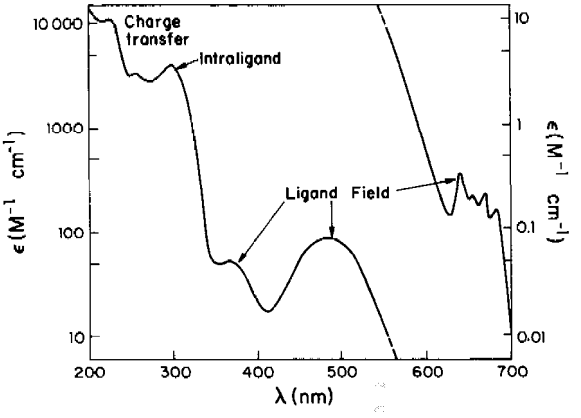

Figure 1 Electronic absorption spectrum of aqueous $[Cr(NCS)(NH_3)_5]^{2+}$ (after Figure 1 in *J. Am. Chem. Soc.*, 1969, **91**, 1076)

$$E = h\nu\,;\ \nu = c/\lambda = c\bar{\nu} \tag{1}$$

$$A = \log(I_0/I) = \varepsilon l C \tag{2}$$

$$f = 4.33 \times 10^{-9} \int \varepsilon(\bar{\nu})\mathrm{d}(\bar{\nu}) \approx 4.6 \times 10^{-9} \varepsilon_{max}\, \bar{\nu}_{1/2} \tag{3}$$

As suggested by Figure 1, the typical absorption band is fairly broad in the case of coordination compounds, and the total transition probability must be obtained by an integration over the whole band. A useful relationship is equation (3),[14] where f is called the transition probability, ε_{max} is the extinction coefficient at the band maximum, and $\bar{\nu}_{1/2}$ is the band width at half-maximum. Values of f range from about 10^8 for a fully allowed transition to a millionfold or so less for a highly forbidden one.

7.3.2.1.1 Ligand field states

Ligand field theory is covered in Chapter 6, and only especially relevant, simple aspects are summarized here. Much of inorganic photochemistry deals with d^3 or d^6 complexes and these two classes will serve as specific examples. The qualitative situation is that the spectroscopic free ion states are split by the electrostatic field of the ligands (the 'ligand field') as illustrated for the d^3 and d^6 cases in Figure 2. Both the one-electron orbital populations and the state designations based on orbital symmetry are shown. Thus for an octahedral (O_h) d^3 complex, the ground state is $^4A_{2g}$, A_2 denoting the orbital symmetry of three unpaired electrons in the t_{2g} (d_{xy}, d_{xz}, d_{yz}) set of orbitals; g indicates that the symmetry is *gerade*, and the left superscript is the spin multiplicity, $m+1$, where m is the number of unpaired electrons. Transitions to the low-lying states $^4T_{2g}$ and $^4T_{1g}$ correspond to the first two broad bands in Figure 1 (assuming effective O_h symmetry) and the weak, highly structured band in the figure corresponds to the transition to ^2E_g.

In the case of an octahedral d^6 complex, the ground state is $^1A_{1g}$ (strong ligand field case), and the first absorption band usually corresponds to the transition to the $^1T_{1g}$ state. There are, in addition, triplet and quintet states which may be low-lying, especially in less symmetric complexes.

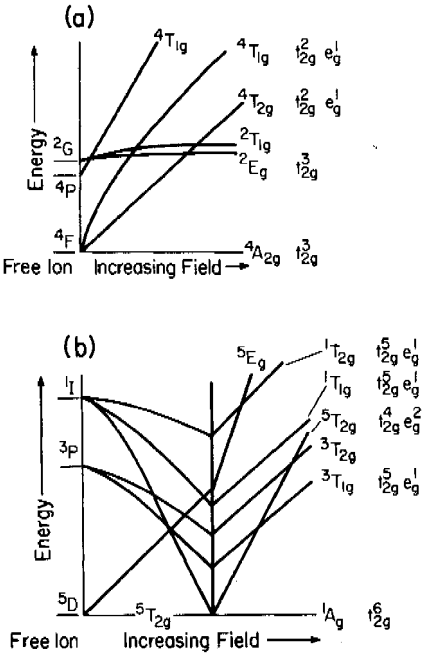

Figure 2 Qualitative energy-level diagrams for (a) d^3 and (b) d^6 transition metals in an octahedral ligand field

Note that the usual, spin-allowed d–d transition places an electron in an $e_g(d_{x^2-y^2}$ or $d_{z^2})$ orbital, which is antibonding. There is a special situation in the d^3 case in that the $^4A_{2g} \rightarrow {}^2E_g$ transition merely rearranges spins in the t_{2g} set of orbitals, which are essentially nonbonding.

In the case of less symmetric complexes, the above states may be split into further ones (except A states), although the basic electron population and the spin designation remain. To avoid dealing with a multitude of term symbols, some authors adopt the practice of designating states as S, D, Q, *etc.*, for singlet, doublet and quartet, with subscripts to be explained in Section 7.3.2.2.1.

7.3.2.1.2 Charge transfer states

Ligand field transitions involve what is essentially an angular rearrangement of electrons. In a molecular orbital diagram, however, one sees that it is possible to move an electron from a metal-centered d orbital to one that is more ligand centered, that is, to make a *radial* change in the electron distribution. We speak of such transitions as charge transfer, CT, with the sub-categories of CTTM for ligand-to-metal, CTTL for metal-to-ligand, CTTS for charge transfer to solvent and LLCT for ligand-to-ligand charge transfer. In the CTTS case, the electron may be ejected into adjacent solvent. Generally speaking, CTTM transitions vary in energy according to the ease of oxidation of the most easily oxidized ligand, while CTTL and CTTS transitions tend to be especially sensitive to the nature of the solvent medium. See ref. 17 for a case of an LLCT transition. CT transitions are often g to u and are relatively allowed (unless there is a spin change); accordingly, ε_{max} values may be several thousand $M^{-1}\,cm^{-1}$, as in the short wavelength band in Figure 1.

7.3.2.1.3 Intraligand states

A free, that is, uncoordinated ligand will have its own absorption spectrum, of course, and features of this spectrum may be seen when the ligand is coordinated, usually red-shifted. In Figure 1, the transition around 305 nm is thought to be primarily an internal thiocyanate transition. Polypyridine and related ligands will often show features derived from the free ligand, as another example.

7.3.2.1.4 Delocalized states

In chelate and macrocyclic complexes, electronic states may exist which are of a delocalized nature; they pertain to the *system* of metal and ligands. Such states are not simply derived from metal d–d states or from free ligand states and transitions involving delocalized states are often quite intense.

7.3.2.1.5 Metal–metal states

Complexes having a direct metal–metal bond will show a corresponding, usually low-energy, absorption band. If metals are connected by bridging ligands, there can be charge transfer excitations, especially if the two metals are in different oxidation states, corresponding roughly to transfer of an electron from one metal to the other.

7.3.2.2 Thexi States and DOSENCO States

7.3.2.2.1 Thexi states

The above discussion has been in relatively spectroscopic terms, the word 'state' implying some specific quantum mechanical designation. An important complication must now be described. Consider first the case of a diatomic molecule in which the internuclear distance is greater in the excited state than in the ground state. As shown in Figure 3, the most probable transition will be from the lowest vibrational level of the ground state, and will be 'vertical'. That is, one accepts the Franck–Condon principle that nuclei do not move appreciably during an electronic transition. The consequence is that the transition will most probably terminate on a high vibrational level of the excited state; we will call this a Franck–Condon (FC) state. The transition energy at the band maximum thus includes a certain amount of vibrational excitation.

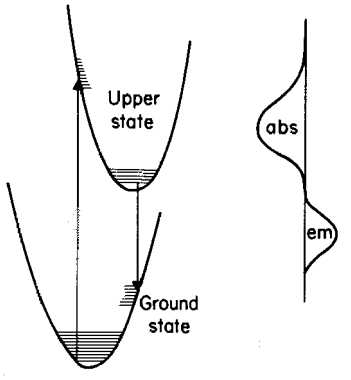

Figure 3 Illustration of vertical transitions during absorption (abs) and emission (em) in a diatomic molecule

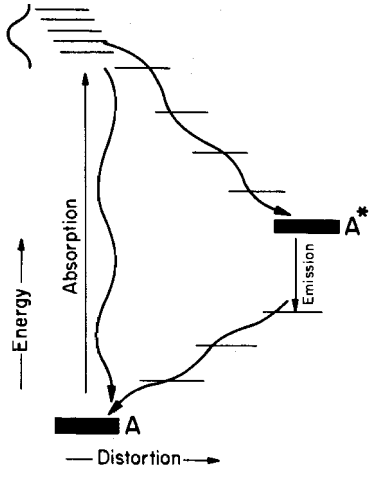

Figure 4 Energy *vs.* distortion diagram (reproduced with permission from *J. Chem. Educ.*, 1983, **60**, 797)

The same situation applies to coordination compounds. It is now impractical to show nuclear coordinates, and in Figure 4 we use the abscissa to denote distortion in a qualitative sense; this may now include bond angle as well as bond length changes. As was noted, the usual d–d transition places an electron in an antibonding orbital, and some geometry change is to be expected. The radial redistribution in a CT transition can likewise distort the excited state potential surface relative to the ground state. Excited state distortion may not be trivial in the case of coordination

compounds. Thus, in the case of square-planar ones, such as $PtCl_4^{2-}$, the excited state is thought to have a distorted tetrahedral geometry.[18]

In solution, the excess vibrational energy following an FC transition is lost very quickly — there are indications that only a few picoseconds are needed for the complex to come to thermal equilibrium with the medium with respect to vibrational excitation.[19] We speak of the *thermally equilibrated excited* state, or, as an abbreviation, of the *thexi* state. Photochemical and photophysical processes very often involve thexi states.

The term 'state' is now being used in a different sense than before. Because of thermal equilibration, we have an electronically excited species that is in thermodynamic equilibrium with its surroundings with respect to vibration (and rotation). We are really talking about an ensemble of species having a Boltzmann distribution of vibrational energy and hence a valid partition function. In brief, a thexi state is a thermodynamic state. It will have an equilibrium structure, a definite absorption spectrum (both UV-visible and IR), well-defined free energy and entropy as well as energy, and well-defined chemistry. It is, in effect, an isomer of the ground state, just as, say, square-planar and tetrahedral forms of a Ni^{II} complex are isomers.

The thermal equilibration of an FC state, while rapid, probably takes place in stages. In solution, a complex is solvated and in a solvent cage. As illustrated in Figure 5, solvent molecules must move to allow the change in geometry to the thexi state. The thin lines of Figure 4 are intended to indicate successive stages of solvent shifting. At each stage, the complex is in a nonequilibrium solvent cage but might have loosely defined vibrational states.

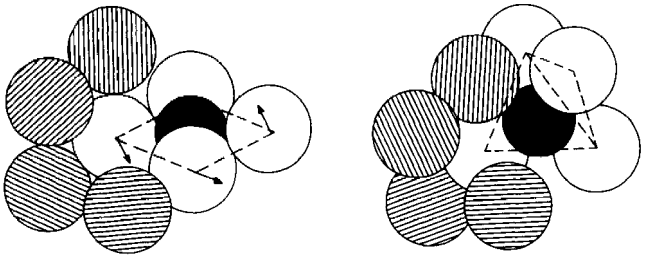

Figure 5 Illustration of solvent cage effect in delaying excited state thermal equilibration (reproduced with permission from *J. Chem. Educ.*, 1983, **60**, 797)

The symmetry-based term symbols used in Section 7.3.2.1.1 are now seen to be potentially misleading; the thexi state geometry may not be that of the ground state. This is the second reason why the nonspecific designations *S*, *D*, *Q*, *etc.* are sometimes used. For a d^3 complex, the ground state becomes Q°_0, the superscript denoting thermal equilibration. The state arrived at following light absorption would be Q_{FC}, and the thermally equilibrated first excited quartet state is Q°_1. The distortion diagram for a d^3 system is depicted in Figure 6. Note that the D°_1 thexi state is shown as little distorted from Q°_0; this is because the electrons have remained in the t_{2g} set of orbitals. Direct evidence for this conclusion will be noted further below.

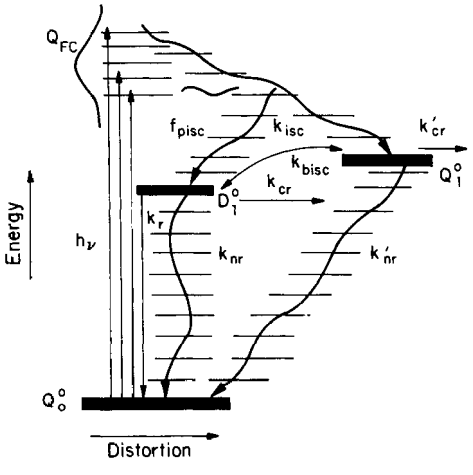

Figure 6 Energy *vs.* distortion diagram for d^3 systems (reproduced with permission from *J. Chem. Educ.*, 1983, **60**, 797)

A final point is that the energy of a thexi state will be less than that of the preceding FC state. The former has been difficult to estimate, but it can be seen from Figures 4 and 6 that it should

correspond roughly to the long wavelength tail of the absorption band. A rule of thumb is to take the wavelength at which ε has dropped to 5% of its maximum value.[20]

7.3.2.2.2 DOSENCO states

There is a possibility that an FC state will react before complete thermal equilibration. In the case of diatomic molecules, the process is usually known as predissociation — a dissociative state crosses the excited state potential surface. The situation is more complicated in the case of a coordination compound, but one can imagine an FC state relaxing along some nuclear coordinate leading to bond breaking. A state capable of such a process has been called a DOSENCO state, an acronym for 'Decay On SElected Nuclear COordinates'.[21] The same authors use the term DERCOS (DEcay *via* Random COordinate Selection) for a thexi state.

7.3.2.3 Kinetics of Excited State Processes

The central process in photochemistry is that of chemical reaction, ordinarily from a thexi state. The quantum yield, ϕ, is defined by equation (4), where n denotes the moles of reaction (corrected for any ground state or thermal reaction) and $\mathscr{E}$ is the einsteins, that is, moles of light quanta absorbed.

The rate processes that must be considered are given by equations (5)–(8). The rate of the process in equation (5) is just that of light absorption by A, I_a. The other three are first order. There may, in addition, be second order processes, of the type given by equation (9), where Q, for quencher, denotes some species that can deactivate A*. Since the concentration of Q, [Q], is usually much larger than [A*], such reactions are pseudo first order.

$$n = \mathscr{E}\phi \tag{4}$$

$$\mathrm{A} \xrightarrow{h\nu} \mathrm{A}^* \tag{5}$$

$$\mathrm{A}^* \xrightarrow{k_{cr}} \mathrm{P} \quad \text{(where P is the photoproduct)} \tag{6}$$

$$\mathrm{A}^* \xrightarrow{k_{nr}} \mathrm{A} \quad \text{(nonradiative return to ground state)} \tag{7}$$

$$\mathrm{A}^* \xrightarrow{k_r} \mathrm{A} \quad \text{(return } \textit{via} \text{ emission of radiation)} \tag{8}$$

$$\mathrm{A}^* + \mathrm{Q} \xrightarrow{k_q} \mathrm{A} + \mathrm{Q} \text{ (or Q*)} \tag{9}$$

If A* is a thexi state, its reactions should obey conventional chemical kinetics, and we can examine several simple, important cases. Suppose firstly that A* is produced by a flash or laser pulse technique in a time short compared to the time scale of the other processes. The produced A* will disappear with a rate constant k which is the sum of the rate constants for all applicable processes. In the absence of quencher, we write $k^\circ = k_{nr} + k_r + k_{cr}$; the time for [A*] to decrease by a factor of e, τ°, is just $1/k^\circ$. With quencher present, we have $k = k_{nr} + k_r + k_{cr} + k_q[\mathrm{Q}]$ and $\tau = 1/k$. The ratio of lifetimes in the absence and presence of quencher is given by equation (10). A plot of τ°/τ *versus* [Q] should thus be linear, with slope $k_q\tau^\circ$; this product is often designated as K_{SV} and called the Stern–Volmer constant.

$$\tau^\circ/\tau = \frac{k_{nr} + k_r + k_{cr} + k_q[\mathrm{Q}]}{k_{nr} + k_r + k_{cr}} = 1 + k_q\tau^\circ[\mathrm{Q}] \tag{10}$$

$$\phi^\circ/\phi = \tau^\circ/\tau = 1 + k_q\tau^\circ[\mathrm{Q}] \tag{11}$$

Since the quantum yield for reaction is simply k_{cr} divided by k° or by k, if Q is present, we also have the relationship in equation (11). Thus the quencher inhibits photochemistry to just the same degree as it reduces the A* lifetime. Since the intensity of emission, I_e, is given by $k_r[\mathrm{A}^*]$, it also follows that I°_e and I_e decay with the lifetimes τ° and τ, and that the ratio I°_e/I_e obeys equation (11).

Consider next the case of a system under steady irradiation, with I_a einsteins of light absorbed per liter per second. We now have the relationship in equation (12). Under steady state conditions, $d[A^*]/dt = 0$, and we can solve equation (12) for $[A^*]$ to give equation (13). The rate of product formation, $d[P]/dt$, is ϕI_a by definition, but is also given by $k_{cr}[A^*]$. These relationships give rise to equation (14). Rearrangement, and taking ϕ° to be the yield in the absence of quencher, gives a result identical to equation (11). The intensity of emitted light is defined as $I_e = \phi_e I_a$ but is also given by $k_r[A^*]$. On combining these statements with equation (11), we obtain equation (15) which is again the Stern–Volmer relationship.

$$d[A^*]/dt = I_a - (k_{nr} + k_r + k_{cr})[A^*] - k_q[Q][A^*] \tag{12}$$

$$[A^*] = \frac{I_a}{(k_{nr} + k_r + k_{cr}) + k_q[Q]} \tag{13}$$

$$d[P]/dt = \phi I_a = \frac{k_{cr} I_a}{(k_{nr} + k_r + k_{cr}) + k_q[Q]} \tag{14}$$

$$I^\circ_e/I_e = \phi^\circ_e/\phi_e = 1 + k_q\tau^\circ[Q] \tag{15}$$

One further case should be examined. Suppose that in equation (9), Q* is formed and is chemically reactive, going to product P′ with a rate constant k'_{cr}. In addition, Q* will have rate constants k'_{nr} and k'_r for nonradiative and radiative relaxation, respectively. The situation is now that light is absorbed by A, but we measure the formation of product P′. We speak of such a process as one of *sensitization*, that is, the formation of P′ is photosensitized by A.

We now ask how the sensitization yield, ϕ_s, varies with [Q], where $d[P']/dt = \phi_s I_a$, and is also given by $k'_{cr}[Q^*]$. For steady-state conditions, the concentration of Q* is given by equation (16). From the definition of ϕ_s and with the use of equation (13), equation (17) is obtained where ϕ_s^∞ is $k'_{cr}/(k'_{nr} + k'_r + k'_{cr})$ and is the yield of P′ at infinite [Q]. From equation (17), a plot of $1/\phi_s$ *versus* $1/[Q]$ should be linear, the intercept and slope allowing calculation of ϕ_s^∞ and K_{SV}.

$$[Q^*] = \frac{k_q[Q][A^*]}{k'_{nr} + k'_r + k'_{cr}} \tag{16}$$

$$1/\phi_s = 1/\phi^\infty_s + \frac{1}{\phi^\infty_s K_{SV}} \frac{1}{[Q]} \tag{17}$$

Processes of the type given by equation (9) are often 'diffusion controlled'. That is, the rate is that at which A* and Q can make diffusional encounters in solution. For room temperature aqueous solution, a typical k_q is in the range 10^9–10^{10} M^{-1} s^{-1}.

Note that in all of these situations, one can begin to unravel the excited state rate constants if measurements of τ° and of τ can be made. There are several ways in which this can be done. The most common one is from the decay of the emission from A*, following pulse excitation. Alternatively, it has been possible in several cases to observe the UV-visible absorption spectrum of A*, and the decay of this absorption again gives τ° or τ (see, for examples, refs. 22–26). In rare cases, it has been possible to observe the rate at which the primary photoproduct P grows in, again following a pulse excitation; it should do this with the lifetime of A*.[27]

There are some additional, useful relationships. Since $\phi^\circ = k_{cr}/(k_{nr} + k_r + k_{cr})$, equations (18) and (19) follow straightforwardly. Thus measurement of τ° and of these yields allows calculation of k_{cr} and of k_r. Radiative relaxation is usually taken to be an intramolecular process whose rate is essentially independent of temperature. If k_r is constant, the relation in equation (20) holds. A common application of this relation is the following. Suppose that I°_e and τ° can be measured at some low temperature, but that at room temperature the k_{nr} and/or k_{cr} processes have become so rapid that τ° is too short to measure. It is sometimes possible, however, to measure I°_e at room temperature in such cases, and, since I°_e and ϕ°_e are proportional, it follows from equation (20) that the expression in equation (21) holds, thus affording an indirect measurement of a lifetime.

$$\phi^\circ = k_{cr}\tau^\circ \tag{18}$$

$$\phi^\circ_e = k_r\tau^\circ \tag{19}$$

$$(\phi^\circ_e/\tau^\circ)_{T_1} = (\phi^\circ_e/\tau^\circ)_{T_2} \tag{20}$$

$$\tau^{\circ}_{T_2} = (I^{\circ}_e)_{T_2}(\tau^{\circ}/I^{\circ}_e)_{T_1} \tag{21}$$

$$D^{\circ}_1 \underset{k_{isc}}{\overset{k_{bisc}}{\rightleftharpoons}} Q^{\circ}_1 \tag{22}$$

To conclude this section, many systems are complicated by the presence of two (or more) low lying states (as in Figure 6). If these states can intercommunicate, one must add to the kinetic scheme various intersystem crossing processes. Thus for the Cr^{III} case, one may need to consider the processes in equation (22), where k_{isc} and k_{bisc} are the rate constants for intersystem crossing and for back intersystem crossing, respectively. The kinetic analysis at this point can become rather complex.[27,28]

7.3.2.4 Electron Distribution and Chemical Reactivity

We turn now to some more detailed considerations of the nature of the various rate processes, beginning with that of chemical reaction of A*. We consider only primary photochemical processes, that is, reactions undergone by A* directly, either uni- or bi-molecularly. The primary photoproduct or products may react further to give the final, observed product but such secondary reactions, while of great importance to the photochemist, are not a principal concern here.

As suggested in the Introduction, the type of excited state A* and the nature of its chemical reactivity often correlate. Thus if A* is a ligand field thexi state, one expects its reactivity to be primarily one of ligand substitution. If A* is a charge transfer state of the CTTM type, one generally observes at least a component of redox decomposition. An example is that of Co^{III} ammine complexes where irradiation in the visible region, where the absorption is of the d–d type, leads to ligand substitution, while irradiation in the UV, where CTTM absorption sets in, leads in part to Co^{II} and oxidized ligand.[13,14] If the absorption is into a CTTL band, a number of reactions can occur and, if into a CTTS band, actual free electron production may be observed. Absorption into an intraligand band is apt to result in ligand-centered chemistry. A thorough treatment of these generalizations is presented in Section 7.3.3.

7.3.2.4.1 Cage mechanism

An early as well as currently useful picture invokes the solvent cage (illustrated in Figure 5).[29,30] If the primary photochemical reaction is one of either homolytic or heterolytic bond fission, the geminal products will tend to remain in the same solvent cage for a few vibrational periods. There will be the possibility of back reaction, either to annul the primary reaction or to allow linkage isomerization.[31] If homolytic bond fission occurs, as with $[CoBr(NH_3)_5]^{2+}$, the Br radical may accept an electron from the Co^{II} moiety before escaping, leading to aquation as the net reaction. If heterolytic bond fission occurs, cage scavenging of the pentacoordinated intermediate would again lead to aquation (or solvation, if in a nonaqueous solvent).

7.3.2.4.2 Photolysis rules and ligand field theory

An early empirical observation with Cr^{III} complexes was that the following rules were obeyed.[7]

(1) Consider the six ligands to lie in pairs at the ends of three mutually perpendicular axes. That axis having the weakest average ligand field strength will be the one labilized, and the total quantum yield will be about that for an O_h complex of the same average ligand field.

(2) If the labilized axis contains two different ligands, then the ligand of greater field strength preferentially aquates. This may be a type of *trans* effect.

As an example, the photochemistry of $[CrCl(NH_3)_5]^{2+}$ is primarily one of ammonia aquation, labelling studies showing that the *trans* ammonia is indeed the one substituted.[32] The photoreaction is *antithermal*; the thermal reaction is entirely one of chloride aquation. The case of $[CrCN(NH_3)_5]^{2+}$ is interesting in that the acido group is a stronger field than ammonia; as predicted by the rules, the photoreaction is one of ammonia aquation, presumably of a *cis* ammonia.[33] While exceptions do exist (*e.g.* *trans*-$[CrF_2(en)_2]^+$),[34] the photolysis rules are qualitatively consistent with the behavior of a large number of mixed-ligand Cr^{III} complexes.

The rules have been accounted for in terms of ligand field theory, taking Q°_1 (see Figure 6) to be the reactive state.[35,36] Figure 7 illustrates the energy level orderings of the one-electron d-orbitals and the electronic states for $[CrX(NH_3)_5]^{2+}$ complexes of effective C_{4v} symmetry. The lowest quartet

excited state is ^4E(a), a component of the $^4T_{2g}$ state in O_h symmetry. Excitation of the complex to ^4E(a) places an electron in a strongly σ-antibonding orbital which is mainly d_{z^2} in character. At the same time a π-antibonding electron has left the t_{2g} set. For purely σ-bonding ligands, such as NH_3, the net effect is to labilize that ligand on the z-axis; the X group is not labilized since it has some π-bonding ability, and thus any σ-bond-weakening effect is partially offset by π-bonding.

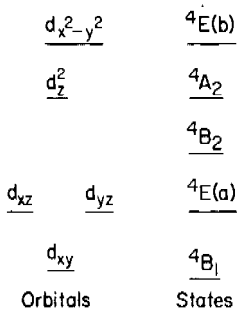

Figure 7 Energy orderings of the orbitals and states of some $[CrX(NH_3)_5]^{2+}$ complexes (X is Cl, Br, NCS) (from ref. 35)

The ligand field treatment has been extended by means of angular overlap calculations and ensuing correlation diagrams.[37] A similar treatment has been made for d^6 complexes, such as those of Co^{III} and Rh^{III}.[38,39] The photolysis rules, incidentally, are not as strongly obeyed with such complexes.

7.3.2.4.3 Environmental effects on photoreactivity

Quantum yields are generally somewhat temperature dependent, but not highly so. Apparent activation energies, E_{act}, in the 8–17 kJ mol^{-1} range are fairly common. Small E_{act} values are not surprising, partly because ϕ is determined by a ratio of rate constants (as in equation 18), and partly on the ground that since excited state lifetimes are short, an A* species will not have time to acquire any large energy of activation before disappearing by some other process. Cases of higher E_{act} values, in the 28–42 kJ mol^{-1} range, have in some cases been attributed to thermally activated intersystem crossing or internal conversion from an unreactive excited state to a higher lying reactive state.[40]

The wavelength dependence of quantum yields tends to be small over the region of absorption to a given type of excited state. Both quantum yield and reaction mode may change considerably, however, if a different type of absorption band is irradiated. The general conclusion is that crossing, particularly between d–d and CT states, is relatively inefficient.

Solvent effects on quantum yields have been studied to some extent. Yields for substitution fall precipitously and the nature of the reaction may change if the medium consists of a noncoordinating solvent. Thus *trans*-$[Cr(NCS)_4(NH_3)_2]^-$ shows a ϕ of about 0.3 in aqueous media (for thiocyanate aquation), but is photoinert in nitromethane. In a mixed solvent study, it was concluded that the photochemical behavior of this complex depended on the solvent composition of the solvation shell rather than on the stoichiometric composition.[41,42]

Some observations have been made on the effect of pressure on quantum yields, using pressures in the 1–2 kbar range.[43–45] Apparent volumes of activation range from about -10 cm^3 mol^{-1} to small positive values for Cr^{III} and Rh^{III} complexes.

7.3.2.4.4 Bimolecular thexi state reactions

There are several categories of reactions of the type represented by equation (9). That of excitation energy transfer has already been noted. Alternatively, the process may be one of electron transfer as in equation (23), with photoexcited $[Ru(bipy)_3]^{2+}$ being the prototypal example of A* and Q being a Co^{III} ammine in the first observed case,[12] but now any of a number of species (see ref. 46 for examples). There has been some success in fitting k_q values to the Marcus treatment of electron transfer rates.[46,47] The reverse of equation (23), that is, excited state reduction, has also been observed. In general, a complex is likely to show excited state electron transfer behavior if it has any accessible one-electron oxidized or reduced forms. The excitation energy of an A* species is usually two or more volts, and this is sufficient to drive a redox reaction that would be highly unfavorable for ground state A.

$$A^* + Q \xrightarrow{k_q} A^+ + Q^- \tag{23}$$

$$AH^* + Q \xrightarrow{k_q} A + QH \quad (24)$$

A third type of bimolecular reaction, summarized by equation (24), is that of excited state proton transfer where Q is now a proton acceptor. This type of process was proposed in the case of the OH^- and CO_3^{2-} quenching of emission from $[RhCl(NH_3)_5]^{2+}$.[48]

Finally, of course, process (9) may not involve any net reaction. In this case the encounter between A* and Q merely results in deactivation of A* to A. The general explanation is along the line that weak interactions during an encounter, especially if Q contains a metal or other heavy atom, can compromise the selection rules that make an A* → A deactivation relatively forbidden.

7.3.2.5 Photophysical Processes

Photophysical processes, that is, ones not involving any change in composition of an A*, have become of much interest to the inorganic photochemist, particularly in terms of excited state kinetic schemes. A brief discussion of the phenomenology and theory of radiative and nonradiative deactivations follows.

7.3.2.5.1 Radiative transitions

The process represented by equation (8), emission from an excited state, is generally called fluorescence if no spin change is deemed to occur, and phosphorescence if there is a spin change. Spin designations can be ambiguous in the case of second and third row transition metal complexes because of the importance of spin–orbit coupling.[49] Most authors retain them, however, as a matter of convention and convenience. A classic case is that shown in Figure 8, for $[Cr(urea)_6]^{3+}$.[50] The broad, long wavelength emission shows a mirror-image spectrum relative to that of the first spin-allowed absorption band, and is taken to correspond to the $Q^\circ_1 \rightarrow Q_{0,\,FC}$ transition ($^4T_{2g} \rightarrow {}^4A_{2g}$ in O_h symmetry), and is termed a fluorescence. Note the considerable Stokes' shift (red shift of fluorescence relative to absorption), indicating that there is significant excited state distortion. The shorter wavelength emission shown in the figure is narrow, and has vibrational structure. It is centered nearly over the doublet absorption band, and is taken to be due to the $D^\circ_1 \rightarrow Q_{0,\,FC}$ transition ($^2E_g \rightarrow {}^4A_{2g}$ in O_h symmetry), and is called a phosphorescence.

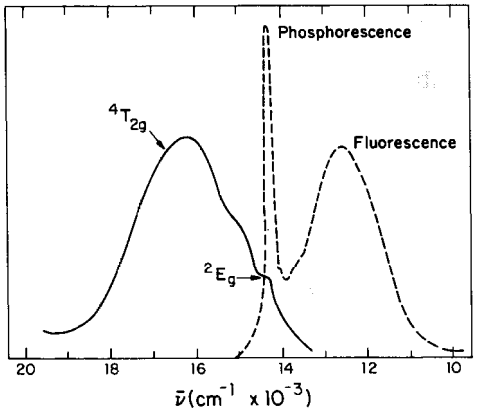

Figure 8 Absorption (—, 298 K) and emission (---, 77 K) spectra of $[Cr(urea)_6]^{3+}$ (after Figure 1 in ref. 50)

Emission from the lowest doublet state is fairly common with Cr^{III} complexes, and often is observable, although weak, in room temperature solution. Typically, τ° values are in the ms range at 77 K and decrease to ns or μs values at room temperature. The low temperature limit is just $1/k_r$; at intermediate low temperatures k_{nr} probably controls τ°, while at room temperature, other processes such as k_{cr} and k_{bisc} are probably controlling. It is this last situation that interests the inorganic photochemist, that is, the behavior of τ° under photochemical conditions. The apparent activation energy may now range up to 40 kJ mol^{-1}, and probably reflects the E_{act} for either the k_{cr} or the k_{bisc} path.

Empirical emission rules for Cr^{III} complexes are the following.[51]

(1) For complexes with six equivalent Cr—L bonds, the emission lifetime in room temperature aqueous solution decreases with decreasing ligand field strength.

(2) If two different kinds of ligand are coordinated, the emission lifetime will be relatively short if that ligand which is preferentially substituted in the *thermal* reaction lies on the weak field axis of the complex. A recent illustration of the application of these rules is with $[CrCN(NH_3)_5]^{2+}$, for which the emission lifetime of 22 μs is indeed relatively long.[52]

Room temperature emission has been observed for a number of transition metal complexes. Examples include Rh^{III} ammines,[53] $[Pt(CN)_4]^{2-}$,[54] and some Cu^{I} phosphine complexes.[55] An important class is that of the polypyridine complexes of Ru^{II} and related species.[56] This last emission, probably from a ^3CT state, is quite strong and its occurrence has made possible a number of detailed studies of electron transfer quenching reactions.

Values of the radiative rate constant k_r can be estimated from the transition probability. A suggested relationship[14,57] is given in equation (25), where n_i is the index of refraction of the medium, $\langle \nu_f^{-3} \rangle$ is the mean of the cube of the reciprocal of the emission frequency, and g_l/g_u is the ratio of the degeneracies in the lower and upper states. It is assumed that the absorption and emission spectra are mirror-image-like and that excited state distortion is small. The basic theory is based on a field wave mechanical model whereby emission is stimulated by the dipole field of the molecule itself. Theory, however, has not so far been of much predictive or diagnostic value.

$$k_r = 2.88 \times 10^{-9} n_i^2 \langle \nu_f^{-3} \rangle^{-1} \int \frac{\varepsilon(\bar{\nu})d\bar{\nu}}{\bar{\nu}} \frac{g_l}{g_u} \tag{25}$$

7.3.2.5.2 Nonradiative transitions

The rate of a nonradiative relaxation such as the k_{nr} process of equation (7) can be estimated from τ° values measured at a sufficiently low temperature such that k_{cr} and k_{bisc} are likely to be unimportant because of their higher activation energy. Under such a condition, $1/\tau^\circ = (k_r + k_{nr})$, and k_r can be estimated from the low temperature limit to τ°, or from equation (25). For coordination compounds, k_{nr} is usually not very temperature dependent, E_{act} typically being 8–12 kJ mol^{-1}.

The process has been treated theoretically in terms of simplified models.[14,58] The quantum mechanics is one of formulating the probability of crossing from an excited to a ground state, summed over all vibrational levels. For coordination compounds, the 'weak' coupling limit is presumably the important approximation. Here, the transition is from low lying vibrational levels of the excited state to very high vibrational levels of the ground state.

The treatment of intersystem crossing, that is, of the k_{isc} and k_{bisc} paths in equation (22), is in principle similar to that for k_{nr}.There is an added spin–orbit coupling term in the evaluation of the electronic factor in the treatment of the crossing probability. Although theory has provided a useful framework for discussing nonradiative processes, it has not so far been of much diagnostic or predictive value in the case of coordination compounds.

7.3.2.6 Chemiluminescence and Triboluminescence

Some mention should be made of ways of producing excited states other than by absorption of light or by excitation energy transfer. A chemiluminescent reaction may be formulated as in equation (26). Since the energy difference between C* and C will be 160 kJ mol^{-1} or more, the corresponding ground state reaction, given by equation (27), must be highly exoergic. As might be expected, the principal examples so far of chemiluminescent reactions involving coordination compounds have been redox ones. An example is presented in equation (28).[59] Both products have emissive excited states, and it is interesting that the actual excited state product is the lower energy one. With other reductants, $[Ru(bipy)_3]^{2+*}$ is formed,[59,60] the reaction with alkaline borohydride providing an excellent lecture demonstration.[61]

$$A + B \rightarrow C^* + D \tag{26}$$

$$A + B \rightarrow C + D \tag{27}$$

$$[Ru(bipy)_3]^{3+} + [Cr(bipy)_3]^{2+} \longrightarrow [Ru(bipy)_3]^{2+} + [Cr(bipy)_3]^{3+*} \tag{28}$$

In triboluminescence, light is produced by grinding or cleaving a solid. Most examples involve organic compounds, but one case of interest here is that of $Ba[Pt(CN)_4]$.[62] A laser-produced shock wave in the solid resulted in population of the emitting excited state.

An important point is that where it has been measured, the emission spectrum produced by either a chemiluminescent reaction or by triboluminescence is the same as that found in the conventional

method of photoexcitation. This is a confirmation that thexi states indeed have thermodynamic status in that their properties are independent of the method of their preparation.

7.3.3 PHOTOCHEMICAL REACTIONS OF COORDINATION COMPOUNDS

The preceding discussion has emphasized that an electronic excited state of a coordination compound is an energy-rich species whose structure, electronic distribution and reactivity can differ substantially from the corresponding properties of the ground state. In this section the reactions of the various types of excited states are considered in detail. Most attention will be given to six-coordinate complexes of metals having a d^3 or low-spin d^6 electronic configuration, since the majority of mechanistic studies reported to date are concerned with these systems. Complexes of other *d* transition elements, the lanthanides and the actinides will also be treated, but the coverage here will necessarily be brief.

7.3.3.1 Ligand Field Excited States

To a first approximation, the ligand field excited states of coordination compounds arise from electronic transitions between valence *d*-orbitals localized on the metal. While such transitions result in an angular rearrangement of metal electron density, they do not alter the net charge distribution between the metal and its ligands. Consequently, ligand field excited states are not expected to undergo intramolecular oxidation–reduction processes such as homolytic fission of a metal–ligand bond. Angular changes in electron density can, however, lead to enhanced reactivity toward ligand substitution and isomerization processes. This theme will be developed in detail below for a number of well-studied transition metal systems.

7.3.3.1.1 Chromium(III) complexes

The low-lying electronic states of six-coordinate Cr^{III} complexes in octahedral (O_h) symmetry are shown in Figure 2a. The $^4A_{2g}$ ground state corresponds, in the strong-field limit, to the t_{2g}^3 electronic configuration whereas the $^4T_{2g}$ and $^4T_{1g}(F)$ ligand field excited states correlate with $t_{2g}^2e_g^1$. Consequently, transitions to these latter states occur with the promotion of an electron to the strongly σ-antibonding e_g orbitals. This redistribution of electron density weakens metal–ligand bonding and can cause considerable distortion of the complex from its original octahedral framework (see Figure 6). Moreover, the vacated t_{2g} orbital is available for bonding to an incoming ligand. These characteristics of the $^4T_{2g}$ and $^4T_{1g}(F)$ excited states make them particularly susceptible to ligand substitution reactions.[35,36] In contrast, the lowest doublet excited state, ^2E_g, arises from a spin-pairing of two electrons within the t_{2g} orbitals. Since these orbitals are nonbonding (except with respect to π-donor or acceptor ligands), this change in electronic distribution should not cause major alterations in metal–ligand bond strength or overall geometry. A recent theoretical study shows, however, that the activation barrier to associative attack by an incoming nucleophile should be lower in ^2E_g than in the ground state.[63] Thus, the lowest doublet state in Cr^{III} complexes must also be considered as potentially reactive toward ligand substitution.

In accord with these expectations, the vast majority of Cr^{III} complexes undergo ligand substitution when irradiated in their ligand field absorption bands.[40] Generally, the leaving ligand is replaced by solvent, although anation may occur at high anion concentration. Complexes having six equivalent metal–ligand bonds, such as $[Cr(NH_3)_6]^{3+}$, undergo initial photosubstitution of a single ligand (equation 29). The analogous process for $[Cr(en)_3]^{3+}$ (equation 30) results in the detachment and protonation of one end of an ethylenediamine ligand (denoted as enH). Thermal cleavage of the second Cr—N bond then yields a mixture of *cis*- and *trans*-$[Cr(en)_2(OH_2)_2]^{3+}$.

$$[Cr(NH_3)_6]^{3+} \xrightarrow[H_3O^+]{h\nu} [Cr(NH_3)_5(OH_2)]^{3+} + NH_4^+ \tag{29}$$

$$[Cr(en)_3]^{3+} \xrightarrow[H_3O^+]{h\nu} [Cr(en)_2(enH)(OH_2)]^{4+} \tag{30}$$

A pulsed-laser photolysis study of $[Cr(en)_3]^{3+}$ illustrates quite dramatically the enhancement in reactivity that can result upon populating a ligand field excited state.[26] Thus a significant fraction of the primary photoproduct, $[Cr(en)_2(enH)(OH_2)]^{4+}$, is formed within the 20 ns duration of the laser pulse and is thought to arise from reaction of the lowest excited quartet state, Q°_1 (see Figure 6). This observation establishes that the pseudo-first-order rate constant for this excited state

process is $\geq 10^8$ s^{-1}. By comparison, the rate constant for the corresponding ground-state thermal reaction is 8×10^{-7} s^{-1} at 25 °C. Thus the promotion of a single electron from the t_{2g} to the e_g orbitals leads, in this case, to a 10^{14} acceleration in the rate of ligand substitution.

Mixed-ligand Cr^{III} complexes have a particularly rich substitutional photochemistry in that two (or more) reaction modes are normally observed. Data for the well-studied class of acidoamine complexes are presented in Table 2. The dominant photochemical reaction for $[CrX(NH_3)_5]^{2+}$ complexes in aqueous solution is NH_3 aquation, with X^- aquation occurring to a lesser extent (equation 31). In contrast, the latter pathway is the favored thermal reaction of these compounds. Such behavior again illustrates that the reactivity of ligand field excited states can differ sharply from that of the ground state.

Table 2 Photochemistry of Mixed-ligand Chromium(III) Complexes upon Irradiation into the Lowest Quartet Ligand Field Band

Complex	$\phi_{NH_3(or\ amine)}$	ϕ_{X^-}	*Major product*	*Ref.*
$[CrCl(NH_3)_5]^{2+}$	0.36	0.005	*cis*-$[CrCl(NH_3)_4(OH_2)]^{2+}$	64
$[CrBr(NH_3)_5]^{2+}$	0.34	0.009	*cis*-$[CrBr(NH_3)_4(OH_2)]^{2+}$	65
$[Cr(NCS)(NH_3)_5]^{2+}$	0.47	0.02	*cis*-$[Cr(NCS)(NH_3)_4(OH_2)]^{2+}$	66
trans-$[CrF_2(en)_2]^+$	0.35	≤ 0.08	$[CrF_2(en)(enH)(OH_2)]^{2+}$	67
trans-$[CrCl_2(NH_3)_4]^+$	0.003	0.44	*cis*-$[CrCl(NH_3)_4(OH_2)]^{2+}$	68
trans-$[CrCl_2(en)_2]^+$	$< 10^{-3}$	0.32	*cis*-$[CrCl(en)_2(OH_2)]^{2+}$	69
trans-$[CrCl_2(2,3,2\text{-tet})]^{+a}$	$< 7 \times 10^{-3}$	0.06	*cis*-$[CrCl(2,3,2\text{-tet})(OH_2)]^{2+}$	70
trans-$[CrCl_2(cyclam)]^{+a}$	$< 2 \times 10^{-4}$	3.3×10^{-4}	*trans*-$[CrCl(cyclam)(OH_2)]^{2+}$	70

[a] 2,3,2-tet is 1,4,8,11-tetraazaundecane; cyclam is 1,4,8,11-tetraazacyclotetradecane.

$$[CrX(NH_3)_5]^{2+} \xrightarrow[H_2O]{h\nu} \begin{cases} cis\text{-}[CrX(NH_3)_4(OH_2)]^{2+} + NH_3 \\ [Cr(NH_3)_5(OH_2)]^{3+} + X^- \end{cases} \quad (31)$$

One of the most controversial questions encountered in studies of Cr^{III} photochemistry concerns the identity of the reactive excited state(s).[71] As illustrated in Figure 6, uncertainty can arise because the Franck–Condon state initially populated during irradiation in the quartet absorption bands generally undergoes rapid equilibration to the lowest thexi quartet state, Q°_1, and/or intersystem crossing to the lowest doublet, D°_1. Reaction from either or both of the latter states must therefore be considered.

In a very important study of the quartet–doublet reactivity question,[72] it was found that ligand-field irradiation of $[Cr(CN)_6]^{3-}$ in degassed dimethylformamide results in both phosphorescence from the doublet and substitution of cyanide. In air-saturated solution, however, phosphorescence is quenched completely while the photoreaction is unaffected. The two processes appear to be uncoupled and thus originate from different excited states. The most straightforward conclusion is that the lowest quartet excited state in $[Cr(CN)_6]^{3-}$ is the sole precursor to photoreaction.

Studies of the photochemistry and photophysics of $[Cr(bipy)_3]^{3+}$, $[Cr(phen)_3]^{3+}$ and various substituted analogues have revealed behavior quite different from that just described.[73] In the prototypal case of $[Cr(bipy)_3]^{3+}$, ligand-field irradiation of the complex in neutral or basic aqueous solution results in phosphorescence and loss of one bipyridine ligand. Intersystem crossing from the lowest quartet state to the luminescent doublet occurs with near unit efficiency, while back-intersystem crossing is too endothermic to be of importance. Addition of 0.1 M iodide ion quenches >99.9% of the phosphorescence and ~98% of the photochemistry. This parallel behavior of the two processes strongly suggests that the quenchable portion of the reaction originates from the doublet.

The issue of quartet *versus* doublet reactivity becomes considerably more complicated for most other Cr^{III} complexes such as $[Cr(en)_3]^{3+}$, *trans*-$[Cr(NCS)_4(NH_3)_2]^-$ and *trans*-$[Cr(NCS)_2(en)_2]^+$. Both phosphorescence and photochemistry can be quenched in these systems, with the former process being affected to a greater degree. While the unquenchable portion of the photochemistry most likely involves prompt reaction from the lowest excited quartet state, the quenchable component could result from either (i) delayed reaction from the quartet following back-intersystem crossing from the doublet, or (ii) reaction from the doublet state itself. Despite a rather extensive series of investigations, the question as to which pathway (i or ii) dominates is still contentious.[40,71]

At present, then, the situation with regard to the identity of the reactive excited state(s) in Cr^{III} substitutional photochemistry can be summarized as follows. The lowest quartet excited state is the sole reactive state in $[Cr(CN)_6]^{3-}$ and is at least partly responsible for the photochemistry of

several other Cr^{III} complexes. The lowest doublet state appears to be the predominant reactive state in $[Cr(bipy)_3]^{3+}$ and similar tris(polypyridyl)chromium(III) complexes and may also be reactive in a number of other complexes. Quite clearly, this aspect of Cr^{III} photochemistry requires additional study.

The photochemical and thermal substitution reactions of Cr^{III} complexes can follow quite different stereochemical courses. The behavior described by equation (32) is typical: thermal aquation of *trans*-$[CrCl_2(en)_2]^+$ proceeds with retention of configuration, whereas photoaquation is accompanied by a highly stereospecific ($\geq 99\%$ *cis* product) rearrangement.[69] With very few exceptions, it has been found that stereochemical mobility is a general feature of Cr^{III} photosubstitution reactions.

$$\textit{trans}\text{-}[CrCl_2(en)_2]^+ \xrightarrow[h\nu]{H_2O} \begin{cases} \textit{trans}\text{-}[CrCl(en)_2(OH_2)]^{2+} + Cl^- \\ \textit{cis}\text{-}[CrCl(en)_2(OH_2)]^{2+} + Cl^- \end{cases} \quad (32)$$

An interesting correlation between the ease of stereomobility during photolysis and the efficiency of photosubstitution has been observed for complexes of the type *trans*-$[CrCl_2N_4]^+$ (Table 2; N_4 is $4NH_3$, 2en, 2,3,2-tet or cyclam).[70] While the overall ligand field strength is approximately constant within the series, the quantum yield for chloride aquation drops by 10^3 as the amine is varied from NH_3 to cyclam. This decrease parallels the increasing chelation about the metal atom. The cyclam complex, in which the metal is completely surrounded by the macrocyclic tetradentate ligand, is remarkably photoinert. Significantly, it is also the only member of the series which cannot undergo stereochemical rearrangement and thus yields the *trans*-chloroaquo complex as the major photoproduct. Though the data base is limited, these results suggest that stereomobility is a necessary condition for efficient substitutional photochemistry in Cr^{III} complexes.

An angular overlap analysis of stereomobility in Cr^{III} photosubstitution reactions has been presented by Vanquickenborne and Ceulemans.[37] In this treatment, the overall reaction is formally dissected into three steps: (1) dissociative loss of a ligand from the lowest quartet excited state of the complex, (2) symmetry-controlled rearrangement of the resulting electronically excited square pyramid to a trigonal bipyramid, (3) symmetry-controlled attack of the incoming ligand on the trigonal bipyramid to yield the final product. Each of these steps is illustrated in Figure 9 for the case of $[CrCl(NH_3)_5]^{2+}$.

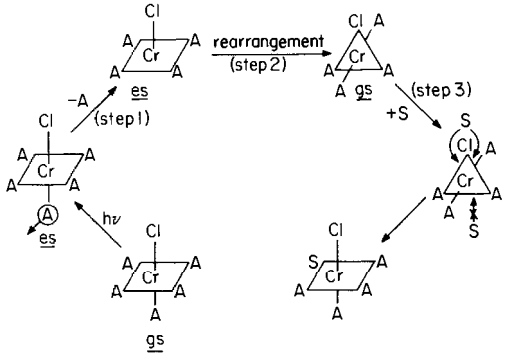

Figure 9 Vanquickenborne–Ceulemans model (see ref. 37) for photosubstitution in $[CrCl(NH_3)_5]^{2+}$; A is NH_3, S is solvent, *gs* and *es* denote ground state and excited state, respectively, and charges are omitted

Extensive comparisons between the stereochemical predictions of this theory and experiment have been presented and, in general, the agreement is satisfactory. Nevertheless, the assumption of dissociative ligand loss (*i.e.* step 1 in Figure 9) is not entirely compatible with other evidence. For example, the quantum yields for anation of $[Cr(DMSO)_6]^{3+}$ by azide are larger than those for anation by thiocyanate at all concentrations, including those that approach limits imposed by ion pairing.[74] This dependence on entering ligand, coupled with the observation that photoanation proceeds more efficiently than photoinduced solvent exchange, is indicative of an associative reaction pathway. In another study,[43] the pressure dependence of photoaquation was determined for $[CrX(NH_3)_5]^{2+}$ (X is Cl, Br or NCS) and $[Cr(NH_3)_6]^{3+}$. The negative volumes of activation found for both NH_3 and X^- loss were interpreted in terms of an I_a (associative interchange) mechanism. The extent of dissociative *versus* associative behavior in Cr^{III} photosubstitution reactions is an interesting and important question that will undoubtedly receive more attention in the future.

Thus far the discussion has focused on the reactivity of the lowest excited states of a given spin multiplicity (*e.g.* $^4T_{2g}$ or ^2E_g in O_h symmetry) since, as noted earlier, higher lying states generally

undergo rapid deactivation by intersystem crossing and/or internal conversion. In some complexes, however, it appears that reaction from upper ligand field thexi states may be competitive with these latter processes. The behavior of *trans*-$[CrF(NCS)(en)_2]^+$ is illustrative in this regard.[75,76] The complex undergoes photosubstitution of both thiocyanate and ethylenediamine with a quantum yield ratio, ϕ_{NCS^-}/ϕ_{en}, that varies with the wavelength of irradiation. This wavelength dependence requires the existence of two reactive excited states, and it was proposed that the $^4E(a)$ and $^4B_2$ states in this nominally C_{4v} complex (see Figure 7) are involved. The $^4E(a)$ state gives rise to both en and NCS^- labilization whereas the higher energy $^4B_2$ state favors en loss. Extension of the Vanquickenborne–Ceulemans photochemical theory[37] to include the reactivity of higher-lying quartet excited states leads to predictions of reactivity which are in accord with the observed behavior.

There are now several reports of a small wavelength dependence of photochemical and emission quantum yields on irradiation into the red edge (long-wavelength portion) of the lowest quartet ligand field absorption band.[77,78] Such behavior has been attributed to prompt intersystem crossing and/or reaction occurring from vibronic levels at or near the Franck–Condon state initially populated during light absorption (see Figure 6). These processes must be extremely rapid (*i.e.* picosecond time scale) to be able to compete successfully with vibrational relaxation to the thexi state. A theoretical treatment of prompt photoreactions has recently been presented.[21]

Finally, it should be noted that the relatively long-lived doublet excited state in Cr^{III} complexes can undergo bimolecular processes of the type mentioned in Section 7.3.2.4.4. Energy transfer is a well-documented[79] pathway for this state and, more recently, electron transfer reactions have also been observed. In the example given by equation (33), the lowest doublet of $[Cr(bipy)_3]^{3+}$ undegoes reductive quenching by $[Ru(bipy)_3]^{2+}$.[80] While this redox process is energetically unfavorable when both reactants are in their ground electronic states, the higher energy of the doublet state provides the necessary driving force to accomplish the reaction photochemically. Additional examples of bimolecular excited state electron transfer processes are presented in Section 7.3.3.2.2.

$$(^2E)[Cr(bipy)_3]^{3+*} + [Ru(bipy)_3]^{2+} \longrightarrow [Cr(bipy)_3]^{2+} + [Ru(bipy)_3]^{3+} \quad (33)$$

7.3.3.1.2 *Cobalt(III), rhodium(III) and iridium(III) complexes*

The energy level diagram for the six-coordinate complexes of Co^{III}, Rh^{III} and Ir^{III} in O_h symmetry is shown in Figure 2b. The $^1A_{1g}$ ground state derives from the t_{2g}^6 electronic configuration, while the low-lying ligand field excited states $^3T_{1g}$, $^3T_{2g}$, $^1T_{1g}$ and $^1T_{2g}$ correlate with the $t_{2g}^5e_g^1$ configuration. There is, in addition, a $^5T_{2g}$ state which arises from the $t_{2g}^4e_g^2$ configuration and whose energy is very sensitive to the ligand field strength. It is generally agreed that the quintet state lies above the $^3T_{1g}$ state in Rh^{III} and Ir^{III} ammine complexes as well as the strong-field complexes of Co^{III} such as $[Co(CN)_6]^{3-}$, whereas the relative positions of these states may be reversed for complexes of lower field strength such as $[Co(NH_3)_6]^{3+}$. This change in the nature of the lowest excited state may account for the different emission properties of the two types of complexes. Thus Rh^{III} and Ir^{III} ammine and Co^{III} cyanide complexes typically exhibit a broad phosphorescence assigned as $^3T_{1g} \rightarrow {}^1A_{1g}$, while Co^{III} ammines are nonemissive even at low temperature.[20]

Table 3 Photosubstitution Quantum Yields for some d^6 Complexes

Complex	λ_{irr}	*Assignment*	$\phi_{NH_3\ (or\ amine)}$	ϕ_{X^-}	*Ref.*
$[Co(NH_3)_6]^{3+}$	365	$^1A_{1g} \rightarrow {}^1T_{2g}$	5.4×10^{-3}	—	82
	460	$^1A_{1g} \rightarrow {}^1T_{1g}$	5.2×10^{-4}	—	
$[Co(CN)_6]^{3-}$	365	$^1A_{1g} \rightarrow {}^1T_{1g}$	—	0.31	83
	405	$^1A_{1g} \rightarrow {}^3T_{1g}$	—	0.29	
$[Rh(NH_3)_6]^{3+}$	254	$^1A_{1g} \rightarrow {}^1T_{2g}$	0.07	—	84
	313	$^1A_{1g} \rightarrow {}^1T_{1g}$	0.075	—	
$[Ir(NH_3)_6]^{3+}$	254	$^1A_{1g} \rightarrow {}^1T_{1g}$	0.083	—	85
	313	$^1A_{1g} \rightarrow {}^3T_{1g}$	0.090	—	
$[RhCl(NH_3)_5]^{2+}$	380	$^1A_1 \rightarrow {}^1T_1$	$<10^{-3}$	0.14	86, 87
$[RhBr(NH_3)_5]^{2+}$	420	$^1A_1 \rightarrow {}^1E$	0.17	0.019	86, 87
$[RhI(NH_3)_5]^{2+}$	420	$^1A_1 \rightarrow {}^1E$	0.87	0.01	86, 87
trans-$[RhCl_2(NH_3)_4]^+$	407	a	$<2 \times 10^{-3}$	0.13	88
trans-$[RhCl_2(en)_2]^+$	407	a	$<3 \times 10^{-3}$	0.057	88
trans-$[RhCl_2(cyclam)]^+$	407	a	$<10^{-4}$	0.011	88

[a] Irradiation into first spin-allowed ligand field absorption band.

Table 3 summarizes the photochemistry of several Co^{III}, Rh^{III} and Ir^{III} complexes upon ligand-field excitation.[81] Ligand substitution is the sole reaction mode and, as shown by equation (34), more than one photoproduct may result for mixed-ligand complexes such as $[RhX(NH_3)_5]^{2+}$ (X is Cl, Br or I). The data reveal an interesting dichotomy between the photoreactivities of Rh^{III} and Ir^{III} ammines and Co^{III} cyanides on the one hand and Co^{III} ammines on the other. The former complexes undergo reasonably efficient substitution and, in most cases, the quantum yields are independent of the irradiation wavelength (λ_{irr}) even in the region corresponding to direct population of the lowest excited triplet state ($^3T_{1g}$ in Figure 2b). Such behavior indicates that photoexcitation is followed by efficient internal conversion/intersystem crossing to a common excited state, logically assigned as the lowest ligand field triplet, and that this state and those in thermal equilibrium with it are mainly responsible for the substitutional chemistry. This conclusion is reinforced by the finding[86] that triplet-state sensitizers drive the reactions in equation (34) with limiting quantum yields that closely match those obtained upon direct photolysis.

$$[RhX(NH_3)_5]^{2+} \xrightarrow[H_2O]{h\nu} \begin{cases} [Rh(NH_3)_5(OH_2)]^{3+} + X^- \\ \textit{trans}\text{-}[RhX(NH_3)_4(OH_2)]^{2+} + NH_3 \end{cases} \tag{34}$$

In sharp contrast, Co^{III} ammines undergo photosubstitution with extremely low and wavelength-dependent quantum yields. Since ϕ values increase with higher-energy excitation, it can be concluded that much of the observed substitutional chemistry arises from higher-lying ligand field excited states. The small photosensitivity of Co^{III} ammines, particularly the lowest-energy excited state, has been attributed to the weak ligand field in these complexes.[20,81] As noted earlier, at sufficiently low field strength the energy of the quintet state, $^5T_{2g}$, falls below that of $^3T_{1g}$. In such cases configurational mixing between $^5T_{2g}$ and the ground state enhances radiationless decay and thus chemical processes (as well as luminescence) will be strongly diminished.[89]

The photosubstitution reactions of Co^{III} and Rh^{III} complexes can occur with a high degree of stereochemical change; some representative examples are presented in equations (35)–(37). Stereomobility during photolysis is not universal, however, as evidenced by the behavior within the series of *trans*-$[RhCl_2N_4]^+$ complexes (Table 3; N_4 is $4NH_3$, 2en or cyclam). Photosubstitution of chloride occurs with complete retention of configuration (equation 38) and, significantly, the quantum yields for this process show much less sensitivity to increasing chelation about the metal than was found for the corresponding Cr^{III} complexes (Table 2). Results such as these demonstrate that stereomobility is not a requirement for efficient photosubstitution in d^6 systems.

$$\textit{cis}\text{- or }\textit{trans}\text{-}[CoCl_2(en)_2]^+ \xrightarrow[H_2O]{h\nu} [CoCl(en)_2(OH_2)]^{2+} + Cl^- \quad (30\%\ \textit{cis} + 70\%\ \textit{trans}) \tag{35}$$

$$\textit{cis}\text{-}[RhCl_2(NH_3)_4]^+ \xrightarrow[H_2O]{h\nu} \textit{trans}\text{-}[RhCl(NH_3)_4(OH_2)]^{2+} + Cl^- \tag{36}$$

$$\textit{cis}\text{- or }\textit{trans}\text{-}[RhCl(OH)(NH_3)_4]^+ \xrightarrow[OH^-]{h\nu} \textit{cis}\text{-}[Rh(OH)_2(NH_3)_4]^+ + Cl^- \tag{37}$$

$$\textit{trans}\text{-}[RhCl_2N_4]^+ \xrightarrow[H_2O]{h\nu} \textit{trans}\text{-}[RhClN_4(OH_2)]^{2+} + Cl^- \tag{38}$$

The photochemical model developed by Vanquickenborne and Ceulemans[39] provides a convenient theoretical framework for discussing the photosubstitutional behavior of d^6 complexes. In this treatment it is assumed that reaction occurs from the lowest triplet state of the complex and that any stereochemical change takes place subsequent to ligand loss. These features are illustrated in Figure 10 for the case of *cis*- and *trans*-$[RhCl_2(NH_3)_4]^+$. For both complexes, angular overlap considerations lead to the conclusion that relative bond strengths lie in the order Rh—N > Rh—Cl. Loss of Cl^- from the triplet state, ^{3}*cis*, of the *cis* isomer produces an electronically excited square-pyramidal intermediate, ^3SP_a, in which the remaining Cl^- lies in the basal plane. Similarly, loss of Cl^- from the triplet state of the *trans* isomer generates ^3SP_b, which contains a Cl^- ligand in the apical position. The square pyramidal intermediates can (i) interconvert along a reaction coordinate that passes through a trigonal bipyramidal transition state of triplet spin multiplicity, ^{3}TBP, or (ii) relax to their respective ground states and add a molecule of solvent. The identity of the final product therefore depends upon the competition between these two pathways. Calculation of relative energies indicates that the ^{3}SP intermediate of lowest energy will be the one having the weaker σ-donor ligand in the apical site and that the barrier for

interconversion, ΔE, becomes larger with increasing ligand field strength. Thus in the example shown in Figure 10, ^3SP_a is predicted to be less stable than ^3SP_b. Isomerization of the former to the latter, followed by deactivation to ^1SP_b and rapid trapping by solvent, would give rise to the observed *trans* product in equation (36). Apparently, ^3SP_b faces too high a barrier (ΔE_T) for conversion to ^3SP_a and, as a result, aquation of the *trans* complex in equation (38) occurs with retention of configuration. High barriers would also account for the observation that most Ir^{III} complexes undergo photosubstitution with stereoretention. The identical product mixtures formed by *cis*- and *trans*-$[CoCl_2(en)_2]^+$ in equation (35), on the other hand, would require that the barriers for interconversion are sufficiently low (because of the smaller ligand field strengths of Co^{III} *versus* Rh^{III} or Ir^{III} complexes) to allow the same steady-state ratio of ^3SP_a and ^3SP_b to be reached by both isomers prior to deactivation and trapping by solvent.

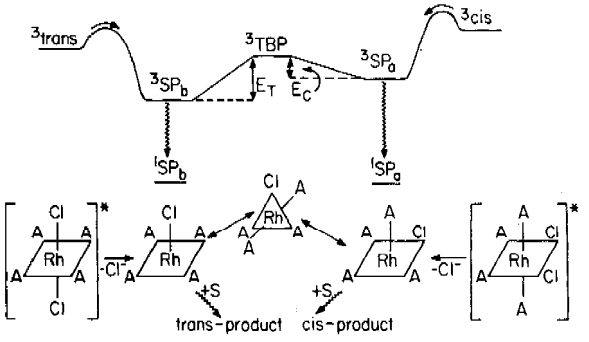

Figure 10. Vanquickenborne-Ceulemans model (see ref. 39) for photosubstitution in *cis*- and *trans*-$[RhCl_2(NH_3)_4]^+$; A is NH_3, S is solvent, and the remaining symbols are defined in the text. Charges on various species have been omitted

While ligand field considerations of the type discussed above usually lead to reliable predictions of photosubstitutional behavior, it is important to note that they are not the only determinant of excited state reactivity. Environmental factors can also play an important role, especially in cases where ligand field effects do not strongly favor one reaction pathway over another. The behavior of $[RhCl(NH_3)_5]^{2+}$ in different solvents illustrates this point;[90] the predominant photoreaction changes from Cl^- loss in water or formamide to NH_3 loss in dimethyl sulfoxide, methanol or dimethylformamide. Measurements of the excited-state rate constants, k_{Cl^-} and k_{NH_3}, for these two processes provide some useful insight about the intimate mechanism of ligand substitution. Thus k_{Cl^-} is found to be much more sensitive than is k_{NH_3} to changes in solvent. Moreover, while neither rate constant correlates with the donor properties of the solvent, k_{Cl^-} qualitatively parallels the solvation energy of the chloride ion. These observations are best interpreted in terms of a dissociative mechanism in which a considerable degree of charge separation develops in the transition state for Rh—Cl bond breaking and the overall energy for this process is influenced by the ability of the solvent to stabilize the developing charge. Other evidence, summarized elsewhere,[81] supports the view that ligand field excited states of d^6 complexes generally undergo ligand substitution *via* a dissociative process.

7.3.3.2 Charge Transfer Excited States

The various categories of CT transitions in coordination compounds were defined in Section 7.3.2.1.2. Such transitions occur with a radial redistribution of electron density and thus cause changes in the oxidation states of the species (metal, ligands, solvent) involved. This property of CT transitions leads to the expectation that the resulting excited states will be particularly susceptible to oxidation–reduction reactions.[91,92] Ligand substitution pathways also may become important, especially in systems where charge transfer creates a substitutionally labile metal center. Likewise, changes in the charge distribution about a coordinated ligand can enhance its reactivity toward processes such as protonation, electrophilic attack and isomerization.

In the acidoammine complexes of Cr^{III}, Co^{III} and Rh^{III}, CT states generally are higher in energy than other types of excited states. This situation is illustrated in Figure 1 for the case of $[Cr(NCS)(NH_3)_5]^{2+}$, where the NCS → Cr CT state is seen to lie above intraligand and ligand field states. Since the CT state reached in absorption can, in principle, relax to any lower energy state, it is often difficult to assign the excited state responsible for a particular reaction. The occurrence of ligand substitution in $[Cr(NCS)(NH_3)_5]^{2+}$ following irradiation of the CT band, for example, could result from reaction of the CT state and/or a lower-lying ligand field state. Another factor that can complicate the interpretation of CT photochemistry is the highly reactive nature of the

primary photoproducts. CT excited states normally react to produce radicals which can undergo secondary reactions with each other, the original complex or the solvent.[91,92] Thus the final products observed may not be a reliable indicator of the nature or the efficiency of the primary photochemical step. Fast-reaction techniques such as laser flash photolysis and pulse radiolysis have been extremely useful in helping to unravel the complex sequence of reactions that can occur in these systems.

7.3.3.2.1 Ligand-to-metal charge transfer states

Most of the available information about the reactivity of CTTM excited states comes from studies of Co^{III} acidoammines.[91,92] Typically, irradiation of a CTTM absorption band in these systems leads to efficient redox decomposition accompanied, in many cases, by ligand substitution or linkage isomerization. The behavior of a representative complex, $[CoCl(NH_3)_5]^{2+}$, is summarized in equation (39).[93] A common observation in these systems is that photoredox quantum yields increase at shorter excitation wavelengths and decrease with increasing solvent viscosity.[91,92]

$$(CTTM)[CoCl(NH_3)_5]^{2+*} \xrightarrow{H_2O} \begin{cases} Co^{2+}_{(aq)} + 5NH_3 + Cl^{\bullet} \\ [Co(NH_3)_5(OH_2)]^{3+} + Cl^- \end{cases} \quad (39)$$

The photochemistry of Co^{III} acidoammines upon CTTM excitation can be understood in terms of a mechanism in which homolytic fission of a metal–ligand bond is the primary reaction.[20,92,94] This process, which produces a solvent-caged or primary radical pair, is shown in equation (40) for the case of $[CoX(NH_3)_5]^{2+}$ (X is Cl, Br, NO_2, NCS). The quantity Δ represents the amount of absorbed light energy in excess of that required for electron transfer, and it determines to a large extent the magnitudes of the kinetic energies of the radical fragments. When Δ is small, recombination of the cage partners is favorable (equation 41a), while for large Δ the radicals are more likely to diffuse apart to form a solvent-separated (S denotes solvent) or secondary radical pair (equation 41b). The secondary radical pair, in turn, can recombine to yield the original complex (or perhaps an isomer; equation 42a), or diffuse apart with or without transfer of an electron back to X (equations 42b and 42c, respectively). The $[Co(NH_3)_5]^{2+}$ fragment produced in equation (42c) is substitutionally labile and rapidly undergoes NH_3 loss to give aquated Co^{2+}.[93] According to this mechanism, photoredox quantum yields increase at shorter excitation wavelengths because of the increasing value of Δ and, hence, the greater likelihood of forming secondary radical pairs. Moreover, a drop in quantum yield with increasing solvent viscosity is expected, since the rates of the processes in equations (41b) and (42c) should decrease in viscous solutions.

$$(CTTM)[(NH_3)_5Co^{III}X]^{2+*} \longrightarrow \{(NH_3)_5Co^{II}, X\cdot\}^{2+}_{\text{solvent cage}} + \Delta \quad (40)$$

$$\{(NH_3)_5Co^{II}, X\cdot\}^{2+} \begin{cases} \longrightarrow [(NH_3)_5Co^{III}X]^{2+} & (41a) \\ \longrightarrow [(NH_3)_5Co^{II}S]^{2+}, X^{\bullet} & (41b) \end{cases}$$

$$[(NH_3)_5Co^{II}S]^{2+}, X^{\bullet} \begin{cases} \longrightarrow [(NH_3)_5Co^{III}X]^{2+} + S & (42a) \\ \longrightarrow [(NH_3)_5Co^{III}S]^{3+} + X^- & (42b) \\ \longrightarrow [(NH_3)_5Co^{II}]^{2+} + S + X^{\bullet} & (42c) \end{cases}$$

The mechanism summarized in equations (40)–(42) is applicable, with some modifications,[92,94] to the CTTM photochemistry of Cr^{III} and Rh^{III} acidoammine complexes. Thus the primary photochemical step is formation of a substitutionally labile reduced metal species and an oxidized ligand radical. In most systems, however, no permanent redox chemistry occurs owing to the facile reoxidation of the metal. The only net photoprocess observed in these cases is substitution of one or more ligands.[70,95]

Bimolecular reactions of CTTM excited states are rare, presumably because of the rapid formation of the primary radical pair in equation (40). In principle, however, it should be possible to intercept the excited state by a reactive species present at sufficiently high concentration in solution. Some evidence for this type of process comes from a study[96] of the photochemistry of $[Mo_2Cl_8]^{4-}$, a complex containing a quadruple metal–metal bond. In strongly acid solution, population of an excited state thought to be CTTM in character results in production of $[Mo_2Cl_8H]^{3-}$. The proposal was made that the increased electron density at the metal centers in this excited state facilitates Mo—H bond formation. Further studies are needed to test the validity of this interesting suggestion.

7.3.3.2.2 *Metal-to-ligand charge transfer states*

Detailed studies of the reactivity of CTTL excited states are of rather recent vintage and have tended to focus on complexes of d^6 metals. This type of state formally contains an oxidized metal center and a reduced ligand radical. In $[Ru(NH_3)_5py]^{2+}$, for example, the low energy Ru → py CT state can be formulated as $[(NH_3)_5Ru^{III}(py^-)]^{2+}$.[97] Several possible reactions can be envisioned for such a species. An intramolecular redox process leading to photooxidation of the metal is one potential pathway, but no net production of Ru^{III} results upon direct CTTL excitation. Another possibility is electrophilic attack by solvent on the reduced pyridine ligand. In acidic D_2O solution, electrophilic H/D exchange of pyridine protons does occur but with a rather small quantum yield ($\sim 10^{-3}$). The only significant photochemical reaction observed in this system is ligand substitution as described by equation (43). It appears unlikely, however, that this pathway originates from the Ru → py CT excited state, since low-spin Ru^{III} complexes (recall the $Ru^{III}(py^-)$ formulation) are known to be relatively substitution inert. Instead, it has been suggested that reaction originates from a ligand field excited state formed by interconversion from the initially populated CTTL state.[97] The situation is depicted schematically in Figure 11.

$$(CTTL)[Ru(NH_3)_5py]^{2+*} \xrightarrow{H_2O} \begin{cases} [Ru(NH_3)_5(OH_2)]^{2+} + py \\ cis\text{- or } trans\text{-}[Ru(NH_3)_4py(OH_2)]^{2+} + NH_3 \end{cases} \quad (43)$$

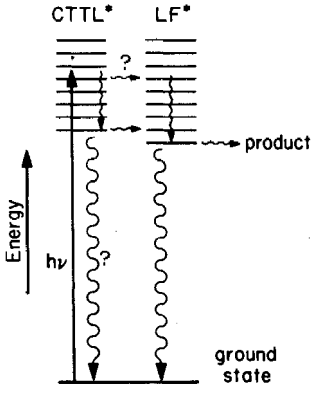

Figure 11 Relative disposition of the metal-to-ligand charge transfer (CTTL) and ligand field (LF) excited state manifolds in $[Ru(NH_3)_5 py]^{2+}$ (after Figure 3 in ref. 98)

Support for this assignment was obtained from a study of the photosubstitutional chemistry of a series of $[Ru(NH_3)_5(pyX)]^{2+}$ complexes, where pyX is a substituted pyridine or related aromatic heterocycle.[98] Systematic variations in the electron withdrawing properties of pyX or, for a given ligand, the solvent polarity were used to 'tune' the energy of the CTTL state relative to the lowest ligand field excited state. When the CTTL state lies above the reactive ligand field state (as in Figure 11), efficient intersystem crossing/internal conversion of the former to the latter results in a relatively high quantum yield for substitution. If the energies of the two states are reversed, however, deactivation leads to population of the unreactive CTTL excited state and the observed quantum yields are low. Similar behavior has been reported for a series of $[Fe(CN)_5L]^{n-}$ complexes (n = 2, 3), where L is an aromatic nitrogen heterocycle.[99]

While intramolecular photoredox reactions of CTTL excited states appear to be relatively unimportant, there is considerable evidence that these states can undergo bimolecular electron transfer with high quantum efficiency.[100–102] Examples of this type of process are given in equations (44) and (45) for the paradigm case, $[Ru(bipy)_3]^{2+}$, a complex possessing a long-lived Ru → bipy CT excited state. The presence of an electron in a high energy π-antibonding orbital of a bipy ligand enhances the reducing ability of this state, while a vacancy (hole) in the t_{2g} metal orbitals increases its oxidizing ability. Thus the excited complex is both a stronger reductant and a stronger oxidant than the corresponding ground state by the excitation energy of 2.1 eV. This behavior is reflected in the reduction potential data shown in Figure 12. Several other transition metal complexes containing long-lived CTTL excited states undergo bimolecular electron transfer processes. The thermodynamic and kinetic aspects of these reactions and their potential applications in energy conversion schemes have been reviewed.[100–102]

$$[Ru(bipy)_3]^{2+*} + Eu^{2+}_{(aq)} \longrightarrow [Ru(bipy)_3]^{+} + Eu^{3+}_{(aq)} \quad (44)$$

$$[Ru(bipy)_3]^{2+*} + Fe^{3+}_{(aq)} \longrightarrow [Ru(bipy)_3]^{3+} + Fe^{2+}_{(aq)} \quad (45)$$

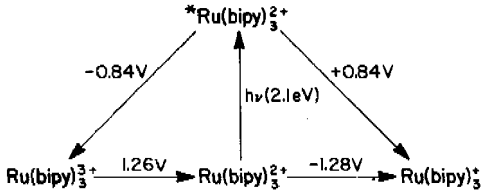

Figure 12 Reduction potentials for various reactions of ground and excited state $[Ru(bipy)_3]^{2+}$ (in H_2O *vs.* NHE)

There are also numerous examples of bimolecular energy transfer processes involving CTTL excited states. The Ru → bipy CT state in $[Ru(bipy)_3]^{2+}$, for example, photosensitizes the reactions of a number of organic and inorganic substrates by this pathway.[103]

Finally, it is conceivable that a CTTL excited state can eject an electron into the solution medium. In systems where this process has been observed, however, it has proved difficult to decide whether the reactive state is CTTL or CTTS in character. A discussion of photoelectron production is presented in the following section.

7.3.3.2.3 Charge-transfer-to-solvent states

CTTS transitions in coordination compounds result in a radial movement of electron density from the metal to the surrounding solution medium. The energies of these transitions generally are very sensitive to environmental parameters such as solvent polarity, temperature and the presence of salts.[104] This sensitivity has been used in a diagnostic sense to identify CTTS bands in the spectra of anionic cyanide complexes[105] and 1,2-dithiolene complexes of Ni, Pd and Pt.[106] Hydrated cations such as $Cr^{2+}_{(aq)}$ and $Fe^{2+}_{(aq)}$ exhibit absorption bands that are sometimes referred to as CTTS in character. Since the solvent occupies the first coordination sphere of the metal, however, the distinction between CTTS and CTTL transitions in these systems becomes obscured.

A characteristic reaction of CTTS excited states is photoelectron production with concomitant oxidation of the metal center.[107] In the example given in equation (46),[108] electrostatic repulsion of the primary photoproducts facilitates their separation and allows direct observation of the solvated electron. In other systems, photoelectron production has been inferred from the products observed in the presence of an electron scavenger such as N_2O or $CHCl_3$.[109]

$$(CTTS)[Ru(CN)_6]^{4-*} \xrightarrow[H_2O]{} [Ru(CN)_6]^{3-} + e^-_{(aq)} \quad (46)$$

$$M^{n+}_{(aq)} + H^+ \xrightarrow{h\nu} M^{(n+1)+}_{(aq)} + \tfrac{1}{2}H_2 \quad (47)$$

UV irradiation of low-valent cations (*e.g.* V^{2+}, Cr^{2+}, Fe^{2+}) in acidic aqueous solution leads to photooxidation of the metal and evolution of H_2.[110] This reaction, described by equation (47), is thought to involve the formation of the oxidized metal and an electron in the primary photochemical act. Immediate scavenging of the photoelectrons by protons yields hydrogen atoms which then combine to produce H_2. Some interest has been shown in this type of system as a component of a photochemical water-splitting cycle.[110,111]

7.3.3.3 Intraligand Excited States

Intraligand (IL) excited states of coordination compounds arise from electronic transitions between molecular orbitals primarily localized on a coordinated ligand. It is difficult, *a priori*, to predict the reactivity of this type of state. While it is logical to expect ligand-centered reactions, the influence of the metal on such processes can be substantial and result in net photochemistry which differs from that of the free ligand. A few examples should serve to illustrate the range of IL photoreactions reported to date.

The complex $[Co(TSC)(NH_3)_5]^{2+}$, where TSC^- denotes *trans*-stilbenecarboxylate, exhibits an absorption band which is virtually identical to the spin-allowed $\pi-\pi^*$ band of free TCS^- and thus is straightforwardly assigned as IL in character.[112] The primary photoreaction upon irradiation into this IL band is redox decomposition to yield aquated Co^{2+} and the radical resulting from

oxidation of TSC^-.[112,113] Photolysis of free TSC^-, on the other hand, results in *trans–cis* isomerization. One possible explanation for this disparate behavior is that the initially populated singlet IL excited state of $[Co(TSC)(NH_3)_5]^{2+}$ undergoes efficient intersystem crossing to a triplet CTTM excited state, from which redox decomposition then occurs. Alternatively, direct transfer of an electron from the locally excited TSC^- ligand to Co^{III} may be occurring. Regardless of the exact details of the mechanism, it is clear that the presence of the metal has a pronounced influence on the reactivity of the IL state.

Metal perturbation of IL photochemistry appears to be less important in $[Ru(bipy)_2(trans\text{-}4\text{-}stilbazole)_2]^{2+}$ and $[Ru(bipy)_2(cis\text{-}4\text{-}stilbazole)_2]^{2+}$. Both complexes undergo wavelength-dependent isomerization of the coordinated stilbazole ligands as the only important photoreaction.[114] This wavelength dependence has been attributed to the presence of two different types of reactive excited states, a Ru → stilbazole CT state which favors formation of the *trans* isomer and a higher energy IL state localized on stilbazole which decays with nearly equal probability to the two isomers. The latter pathway is qualitatively similar to the isomerization process that obtains upon direct photolysis of the free ligand. Thus coordination to Ru has not altered the characteristic photoreaction mode of the stilbazole molecule.

Photolysis of aqueous solutions of $[RhN_3(NH_3)_5]^{2+}$ and $[IrN_3(NH_3)_5]^{2+}$ results in the evolution of N_2 and the formation of a coordinated nitrene (M—NH) intermediate.[115,116] This cleavage of the $N—N_2$ bond originates primarily from an IL excited state localized on the azide ligand.[115–117] The metal is thought to play an important chemical role in the excited state reaction by stabilizing the incipient nitrene through a $d_\pi - p_\pi$ backbonding interaction.

7.3.3.4 Survey of the Photoreactions of *d* and *f* Transition Metal Complexes

The preceding discussion of the relationships between excited state electronic structure and photochemical reactivity focused primarily upon coordination compounds containing d^3 or low-spin d^6 transition metals. These relationships are generally applicable, however, to complexes of other *d* transition elements, the lanthanides and the actinides. A brief survey of the photochemical reactions of these latter systems is presented below.

7.3.3.4.1 Complexes of d *transition elements*

Several coordination compounds in which the central metal possesses a high oxidation state and a d^0 electronic configuration have been reported to undergo photoinduced homolytic cleavage of a metal–ligand bond, presumably the result of populating a CTTM excited state. UV or visible irradiation of $TiCl_4$, for example, causes homolysis of a Ti—Cl bond with the resulting formation of $TiCl_3$ and Cl_2.[118] Vanadium complexes of general formula $VOQ_2(OR)$, where Q is the 8-quinolyloxo ligand and R is an alkyl group, undergo cleavage of the V—OR bond upon UV photolysis.[119] This reaction occurs for a wide selection of R groups and thus provides a convenient, general route to alkoxy radicals.

The eight-coordinate d^2 complexes $[Mo(CN)_8]^{4-}$ and $[W(CN)_8]^{4-}$ undergo two wavelength-dependent photoreactions. Photolysis in the short-wavelength (254 nm) region leads to efficient photoelectron production from an excited state assigned as CTTS in character.[107,108,120] Irradiation into the longer-wavelength (365 nm) ligand field bands, on the other hand, favors ligand substitution.[121–123] As described by equation (48), the primary substituted photoproduct in basic media is the hydroxo complex which, in a series of thermal reactions, undergoes additional release of cyanide.

$$[M(CN)_8]^{4-} \xrightarrow[OH^-]{h\nu} [M(CN)_7(OH)]^{4-} + CN^- \tag{48}$$

In the dinuclear complex $[Re_2Cl_8]^{2-}$, the d^4 metal centers are linked by a quadruple bond. The lowest-lying singlet excited state in the complex arises from the $\delta-\delta^*$ transition of the Re_2 unit.[124] This state has been found to undergo bimolecular electron transfer with a variety of substrates in acetonitrile solution, functioning either as a strong oxidant or a moderately good reductant.[125] Population of higher-energy excited states results in cleavage of the Re—Re bond and formation of monomeric $[ReCl_4(MeCN)_2]^-$.[126] In the absence of evidence for direct photodissociation of the quadruple bond, it was proposed that this reaction proceeds by way of an intermediate in which a chloride ligand bridges the two metal atoms. Since this type of structure leaves one of the Re atoms quite exposed to the environment, nucleophilic attack by solvent can assist the Re—Re bond rupture process.

Low-spin d^5 complexes possess a CTTM excited state that arises from the transfer of a ligand electron to a metal orbital having predominantly nonbonding (t_{2g}) character. In $[RuCl(NH_3)_5]^{2+}$, for example, the Cl → Ru CT state can be conceptualized as a Ru^{II} complex containing a bound ligand radical. Since the substitutional lability of Ru^{II} complexes is not especially great, this state might be expected to undergo internal back-electron transfer to regenerate the original complex faster than it decomposes to redox products. This expectation is borne out by the observation that CTTM excitation of $[RuCl(NH_3)_5]^{2+}$ leads to relatively inefficient ($\phi = 0.02$–0.04) loss of NH_3 as the only net photoprocess.[127] Similar considerations account for the lack of CTTM photochemistry for $[IrCl_6]^{2-}$.[128] Ligand field excitation of d^5 complexes generally results in ligand substitution and/or isomerization processes. As summarized in equation (49), photolysis of *cis*- or *trans*-$[RuCl_2(en)_2]^+$ leads to an isomeric mixture of the chloroaquo products but, interestingly, the isomer distribution differs for the two starting complexes.[129] This behavior has been analyzed in terms of the angular overlap model of ligand field photochemistry.[130]

$$\begin{array}{ccccc} & & cis\text{-}[RuCl(en)_2(OH_2)]^{2+} & & \\ & \overset{h\nu}{\underset{H_2O}{\uparrow 84\% \atop \downarrow 16\%}} & & \overset{h\nu}{\underset{H_2O}{\uparrow 66\% \atop \downarrow 34\%}} & \\ cis\text{-}[RuCl_2(en)_2]^+ & & & & trans\text{-}[RuCl_2(en)_2]^+ \\ & & trans\text{-}[RuCl(en)_2(OH_2)]^{2+} & & \end{array} \qquad (49)$$

While four-coordinate d^8 complexes of Pt^{II} are square planar in their ground electronic states, spectroscopic[131,132] and theoretical studies[133] suggest that the low-lying ligand field excited states are significantly distorted and may even approach tetrahedral geometry. Minimally, such distortion provides a ready pathway for isomerization, and can also result in labilization of specific metal–ligand bonds. Consider the example of Zeise's anion, $[PtCl_3(C_2H_4)]^-$, which in the ground state undergoes rapid aquation of the chloride *trans* to ethylene. Ligand field excitation results in substitution of both *cis*-chloride and ethylene (the extent of *trans*-chloride photoaquation could not be determined).[18] The photolability of ethylene was attributed to the distortion of ligand field excited states toward a tetrahedron, since in this geometry π-backbonding from Pt to C_2H_4 is weakened relative to that in the square planar ground state. Several Pt^{II} complexes undergo *cis–trans* isomerization when irradiated in their ligand field absorption bands,[134] specific examples being $[PtCl_2(PEt_3)_2]$,[135] $[Pt(gly)_2]$ (gly is glycinate)[136] and $[Pt(py)_2Cl_2]$.[137] The first two systems are thought to isomerize *via* an intramolecular twisting mechanism, whereas a combination of intramolecular twisting and intermolecular ligand substitution pathways is responsible for the rearrangement of the last complex.

In solution the d^8 complexes of Ni^{II} are characterized by several rapid equilibria between species having different coordination numbers and/or geometries. Upon irradiation, these equilibria are perturbed and can be studied by relaxation techniques. A number of photoinduced changes have been investigated in this manner including square planar/tetrahedral, four-coordinate/five-coordinate and four-coordinate/six-coordinate interconversions.[138]

The photochemistry of d^9 Cu^{II} and d^{10} Cu^{I} complexes is dominated by redox processes.[139] Halide complexes of general formula $[CuCl_x]^{(2-x)-}$ or $[CuBr_x]^{(2-x)-}$ ($x = 1$–4), for example, undergo intramolecular electron transfer of the CTTM type to form a reduced metal species and a free halogen atom.[140,141] CTTM photochemistry has also been observed for Cu^{II} complexes containing amines, carboxylates, β-diketonates or polypyridines.[139] Copper(I) halide complexes such as $[CuCl_3]^{2-}$ undergo photoelectron production, presumably the result of populating a CTTS excited state.[142,143] In acidic aqueous media, scavenging of the electron by H^+ results in evolution of H_2. Irradiation of $[Cu(dmp)_2]^+$ (dmp is 2,9-dimethyl-1,10-phenanthroline) populates a low-lying CTTL excited state which can undergo bimolecular electron transfer to various Co^{III} complexes.[144] Photoinduced intramolecular electron transfer from Cu^{I} to Co^{III} in a mixed-metal dimer has also been reported.[145] Finally, [Cu(prophos)BH_4] (prophos is 1,3-bis(diphenylphosphino)propane) has been shown to undergo bimolecular energy transfer to organic substrates in solution from an IL excited state localized on the prophos ligand.[146]

7.3.3.4.2 Complexes of the lanthanide and actinide elements

Most of the reported photochemical reactions of lanthanide complexes involve some type of redox behavior.[147] Photolysis (254–405 nm) of Eu^{2+} in acidic aqueous solution, for example, results in photooxidation of the metal and generation of H_2 (equation 50).[148] While the excited states responsible for this reaction nominally arise from $4f \rightarrow 5d$ transitions localized on the metal, strong mixing of the 5*d*-orbital with ligand orbitals endows these states with appreciable CTTL character. Photoreduction of aquated Eu^{3+} can also be driven with UV ($\leqslant 254$ nm) light[149] and forms the

basis of a photochemical separation of europium from other trivalent lanthanide elements.[150] The primary photoreaction, summarized in equation (51), is consistent with the population of a CTTM state. Several photoredox processes involving the Ce^{4+}/Ce^{3+} couple have been reported. Examples include bimolecular electron transfer from the $4f \rightarrow 5d$ excited state of Ce^{3+} to Cu^{2+} in aqueous solution[151] and the Ce^{4+}-mediated oxidation of organic substrates such as alcohols, acids, aldehydes and ketones.[152]

$$Eu^{2+}_{(aq)} + H^+ \xrightarrow{h\nu} Eu^{3+}_{(aq)} + \tfrac{1}{2}H_2 \tag{50}$$

$$Eu^{3+}_{(aq)} + H_2O \xrightarrow{h\nu} Eu^{2+}_{(aq)} + H^+ + \cdot OH \tag{51}$$

A few observations of photosubstitution in lanthanide complexes have been reported. Irradiation into the f–f bands of $[Pr(thd)_3]$, $[Eu(thd)_3]$ and $[Ho(thd)_3]$ (thd is the anion of 2,2,6,6-tetramethyl-3,5-heptanedione) results in substitution of thd by solvent.[153] The proposed mechanism involves intramolecular energy transfer from an f–f excited state to a reactive IL excited state which is responsible for the observed ligand loss. Photosubstitution has also been observed upon direct excitation into the ligand absorption bands of $[Tb(thd)_3]$.[154]

Knowledge of actinide photochemistry is limited mainly to the complexes of uranium,[155] especially those containing the uranyl ion, UO_2^{2+}.[100,156,157] The lowest excited state of this ion is associated with a transition from essentially nonbonding π-orbitals to empty $5f$-orbitals on the U atom.[158] This state has been found to undergo a variety of bimolecular reactions. Upon irradiation in aqueous solutions of primary and secondary alcohols, for example, UO_2^{2+} abstracts a hydrogen atom from the α-carbon atom of the alcohol (equation 52).[159–161] The resulting U^V species deprotonates and then undergoes disproportionation to UO_2^{2+} and U^{4+}. Bimolecular electron transfer to photoexcited UO_2^{2+} from a variety of electron donors is now well documented,[162–164] and a few examples of bimolecular energy transfer have also been reported.[165,166] Complexes of UO_2^{2+} with several carboxylic acids or their conjugate bases possess reactive CTTM excited states which lead to reduction of the metal and oxidation of the organic moiety. The best known example is UO_2^{2+} oxalate,[167] since this system has found use as a chemical actinometer.[168]

$$UO^{2+}_{2(aq)} + R^1R^2CH(OH) \xrightarrow{h\nu} UO_2H^{2+}_{(aq)} + R^1R^2\dot{C}(OH) \tag{52}$$

Interest in the reprocessing of spent nuclear fuels has prompted studies of the solution photochemistries of Np and Pu. A recent review summarizes the photoredox behavior of the various oxidation states of these elements.[169]

7.3.4 APPLICATIONS OF PHOTOCHEMICAL REACTIONS OF COORDINATION COMPOUNDS

In this final section we turn our attention to some applications of inorganic photochemical reactions. One obvious and immensely important example, treated in Chapter 59, is the use of metal-based (particularly silver) systems in photographic processes. Additional applications occur in the area of solar energy conversion and storage. As discussed in Chapter 61.5, a variety of schemes for photochemical water-splitting make use of transition metal photoredox reactions. Other energy storage processes such as the production of highly strained organic molecules, the photoreduction of carbon dioxide and the generation of electricity in photogalvanic or photoelectrochemical cells also incorporate inorganic photochemical steps.[170–173] Several applications of inorganic photoreactions that are not treated elsewhere in this compendium are described below.

7.3.4.1 Synthesis and Catalysis

Photochemical reactions have been exploited to yield coordination compounds that are otherwise difficult to prepare. For example, mixed-ligand complexes of general formula *trans*-$[MClX(en)_2]^+$ (M is Rh or Ir; X is Br or I) can be obtained in high yields by initial photochemical conversion of aqueous *trans*-$[MCl_2(en)_2]^+$ to the corresponding chloroaquo complex as described in equation (53).[174] Precipitation of free Cl^- with Ag^+ followed by heating with one equivalent of X^- then yields the desired product. Thermal routes to these complexes are less desirable because of the propensity to form disubstituted products and the need for extended

reaction times at high temperatures. Photosubstitution reactions are also employed in the syntheses of a large number of $[RuX(bipy)_2L]^+$ and $[RuX_2(bipy)]$ complexes, where L is an uncharged ligand such as py or CH_3CN and X^- is an anion such as ClO_4^-, NO_3^-, Br^- or Cl^-.[175] Additional examples of synthetic applications of inorganic photochemistry have been described.[176]

$$trans\text{-}[MCl_2(en)_2]^+ \xrightarrow{h\nu} trans\text{-}[MCl(en)_2(OH_2)]^{2+} + Cl^- \tag{53}$$

$$O \xrightarrow[M]{h\nu} O' \tag{54}$$

Organic molecules can undergo an assortment of fundamentally interesting and synthetically useful transformations when irradiated in the presence of coordination compounds. The generic process is represented by equation (54) where O and O′ denote the original and transformed organic substrate, respectively, and M symbolizes a transition metal compound normally present in catalytic amount. Among the classes of organic substrates reported to engage in this type of process are alkenes, aldehydes, ketones, acids, ethers, epoxides, alcohols, nitriles and various aromatics. Reaction types include isomerization, cycloaddition, polymerization, hydrogenation and oxidation.

The transformation shown in equation (54) retains many of the features of ordinary photochemical and transition-metal-catalyzed thermal reactions of organic compounds, but displays some unique characteristics as well. In cases where irradiation serves only to accelerate the rate of the expected thermal process, higher chemical yields of product can result, reaction rates are subject to greater control through regulation of light intensity, and thermally sensitive products are isolated more readily since elevated reaction temperatures can be avoided. Alternatively, the function of M may be to facilitate known photochemical reactions of O or perhaps introduce new reaction channels not observed upon irradiation of O alone. A detailed discussion of the mechanisms and synthetic applications of these processes has been presented.[177]

7.3.4.2 Chemical Actinometry

The accurate determination of incident light intensity is of pivotal importance in any quantitative photochemical experiment. While various physical devices are available for making absolute intensity measurements,[168] these devices can be difficult to calibrate and usually are rather expensive. A much simpler approach involves the use of a chemical actinometer. This type of system is based upon a photochemical reaction for which product quantum yields are reasonably insensitive to variations in reactant concentration, temperature, light intensity and excitation wavelength. Once the quantum yield is calibrated by an absolute method, a chemical actinometer becomes a rapid, inexpensive and highly accurate secondary standard for light intensity measurements.

Most solution-phase actinometers in use today are based upon the photochemical reactions of coordination compounds. The redox decomposition of acidic solutions of $[Fe(C_2O_4)_3]^{3-}$, for example, is very sensitive to light in the range 254–500 nm.[168] A very good actinometer for longer wavelengths (316–750 nm) involves the photoaquation of *trans*-$[Cr(NCS)_4(NH_3)_2]^-$ (the anion of Reinecke's salt).[178] The extent of reaction in these systems is determined spectrally following the addition of a reagent which forms a highly absorbing complex with one of the photoproducts.

A chemical actinometer especially designed for intensity measurements on high power lasers in the 330–520 nm range has been described.[179] It consists of a closed O_2-filled system containing methanolic $[Ru(bipy)_3]^{2+}$ and tetramethylethylene (TME). Photoexcited $[Ru(bipy)_3]^{2+}$ is quenched efficiently by dissolved O_2 to generate singlet oxygen which then reacts with TME to form a nonvolatile hydroperoxide. The laser intensity is determined from the rate of O_2 consumption monitored on a gas buret.

Finally, the photoredox decomposition of $K_3[Mn(C_2O_4)_3]\cdot 3H_2O$ has been proposed for use as an actinometer for solid state photochemical studies.[180] Upon UV irradiation, the crystals of this complex change from deep red to white and the extent of reaction can be measured easily by reflectance spectroscopy.

7.3.4.3 Photochromism

Photochromism may be defined as the reversible light-induced interconversion of a system between two forms having distinguishably different absorption spectra.[181] The generalized process is outlined in equation (55) where ϕ represents the quantum yield for photochemical reaction and

k denotes the rate constant for the corresponding thermal process. When the combined (photochemical + thermal) rate of the back reaction equals that of the forward process, the system attains a photostationary state. In the case where $\phi_A \gg \phi_B$ and $k_B \gg k_A$, only the photochemical forward reaction and thermal reversion need to be considered and the system is termed singly photochromic.

$$A \underset{\phi_B, k_B}{\overset{\phi_A, k_A}{\rightleftharpoons}} B \tag{55}$$

The typical response of a singly photochromic system to light is depicted in Figure 13.[182] Initially, only form A is present, but upon exposure of the system to irradiation at time t_1, the photochemical conversion of A to B ensues. The B/A ratio thus increases until it attains the equilibrium value of the photostationary state. Upon removal of the light source at time t_2, the photoreaction ceases and B reverts to A at a rate characteristic of the thermal back reaction. The potential commercial and military applications of such reversible light-sensitive materials have provided much of the impetus for research on photochromic behavior. A partial listing of applications includes chemical switches, data displays, information storage, radiation intensity control (*e.g.* sunglasses) and camouflage.[183]

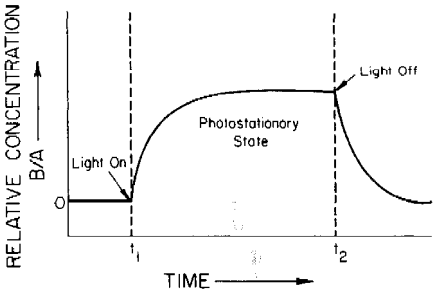

Figure 13 Response of a singly photochromic system to light; irradiation commences at time t_1 and ends at t_2

The majority of inorganic systems reported to exhibit photochromism are solids, examples being alkali and alkaline earth halides and oxides, titanates, mercuric chloride and silver halides.[184,185] The coloration is generally believed to result from the trapping of electrons or holes by crystal lattice defects. Alternatively, if the sample crystal is doped with an impurity capable of existing in variable oxidation states (*i.e.* iron or molybdenum), an electron transfer mechanism is possible.

In solution the photochromism of coordination compounds can result from photoinduced isomerization (*e.g.* metal dithizonates[186–188]), substitution (*e.g.* iron(II) phthalocyanine in the presence of benzyl isocyanide[189]) and oxidation–reduction (*e.g.* tris(diethyldithiocarbamato)-nickel(IV) bromide[190]).

7.3.4.4 Photocalorimetry

Photocalorimetry is a technique for determining the ordinary enthalpy (ΔH) of a reaction but, unlike conventional calorimetry, the reaction is light induced.[191] Essentially, the procedure involves measuring the rates of heat production in two irradiated solutions, one containing an absorbing but unreactive substance and the other containing the photosensitive compound. The difference between these rates, per mole of reaction, gives the ΔH for the photochemical process.

Photocalorimetry offers a convenient alternative to other methods of ΔH determination and, in some instances, may be the only practical method. The ligand substitution reactions of robust Werner-type complexes are a case in point. Conventional thermochemical measurements are complicated by the slowness of the substitution process and/or by competing reactions. Some of these same complexes, however, undergo clean photosubstitutions with high quantum yields and thus are excellent candidates for photocalorimetry. Examples include $[Cr(NH_3)_6]^{3+}$, $[Cr(CN)_6]^{3-}$ and $[Co(CN)_6]^{3-}$.[192] Photocalorimetric measurements of ΔH have also been obtained for isomerization and redox reactions of coordination compounds.[193,194]

7.3.5 ADDENDUM

The field of inorganic photochemistry continues to grow at a rapid pace. Summarized below are several interesting articles that have appeared since the original submission of this chapter.

Additional studies addressing the issue of doublet *vs.* quartet state reactivity in Cr^{III} complexes have been reported.[195–197] Factors affecting the nature and lifetime of the phosphorescent state

in Cr^{III} ammines have been discussed.[198,199] The macrocyclic complex *trans*-$[Cr(CN)_2(cyclam)]^+$ was found to be photoinert and to possess a long-lived and relatively temperature independent phosphorescence;[200] these characteristics make it an attractive candidate for studies of bimolecular electron transfer and energy transfer processes.

Efforts continue to elucidate the excited-state dynamics and ligand substitutional reactivities of d^6 transition metal complexes.[201–203] Fluorescence from incompletely relaxed ligand field singlet states has been detected for some haloamminerhodium(III) complexes.[204]

Evidence continues to mount in support of the view that the optically excited electron in the metal-to-ligand charge transfer excited state of $[Ru(bipy)_3]^{2+}$ and related complexes resides on a single ligand ring.[205–208] Reviews dealing with bimolecular excited-state electron transfer reactions of d^6 metal–polypyridyl complexes have appeared.[209,210] Orthometallated Ir^{III} complexes containing one or more metal–carbon bonds possess some interesting properties including the ability to act as powerful excited-state reductants.[211,212] The excited-state redox properties of binuclear[213–215] and polynuclear[216] complexes containing metal–metal bonds have been investigated.

Studies of inorganic photochemistry in unusual environments has attracted considerable attention. Photochemical studies conducted in organized assemblies such as micelles, microemulsions and vesicles,[217] on surfaces such as porous Vycor glass,[218] in a lamellar solid,[219] and in the gas phase have been reported.[220]

Finally, two reviews have appeared describing the applications of inorganic photochemistry in the sensitization and/or catalysis of organic reactions.[221,222]

7.3.6 REFERENCES

1. J. Eder, *Ber.*, 1880, **13**, 166.
2. W. G. Leighton and G. S. Forbes, *J. Am. Chem. Soc.*, 1930, **52**, 3139.
3. J. Vranek, *Z. Elektrochem.*, 1917, **23**, 336.
4. R. Schwartz and K. Tede, *Ber.*, 1925, **58B**, 746.
5. M. Linhard and M. Weigel, *Z. Anorg. Allg. Chem.*, 1951, **266**, 49.
6. E. H. Archibald, *J. Chem. Soc.*, 1920, 1104.
7. A. W. Adamson, *J. Phys. Chem.*, 1967, **71**, 798.
8. A. W. Adamson, W. L. Waltz, E. Zinato, D. W. Watts, P. D. Fleischauer and R. D. Lindholm, *Chem. Rev.*, 1968, **68** 541.
9. A. Vogler and A. W. Adamson, *J. Am. Chem. Soc.*, 1968, **90**, 5943.
10. N. A. P. Kane-Maguire and C. H. Langford, *Chem. Commun.*, 1971, 895.
11. S. Chen and G. B. Porter, *Chem. Phys. Lett.*, 1970, **8**, 41.
12. H. D. Gafney and A. W. Adamson, *J. Am. Chem. Soc.*, 1972, **94**, 8238.
13. V. Balzani and V. Carassiti, 'Photochemistry of Coordination Compounds', Academic, New York, 1970.
14. A. W. Adamson and P. D. Fleischauer (eds.), 'Concepts of Inorganic Photochemistry', Wiley, New York, 1975.
15. M. Wrighton, *Chem. Rev.*, 1974, **74**, 401.
16. G. L. Geoffroy and M. S. Wrighton, 'Organometallic Photochemistry', Academic, New York, 1979.
17. A. Vogler and H. Kunkely, *J. Am. Chem. Soc.*, 1981, **103**, 1559.
18. P. Natarajan and A. W. Adamson, *J. Am. Chem. Soc.*, 1971, **93**, 5599.
19. A. D. Kirk, P. E. Hoggard, G. B. Porter, M. G. Rockley and M. W. Windsor, *Chem. Phys. Lett.*, 1976, **37**, 199.
20. P. D. Fleischauer, A. W. Adamson and G. Sartori, *Prog. Inorg. Chem.*, 1972, **17**, 1.
21. B. R. Hollebone, C. H. Langford and N. Serpone, *Coord. Chem. Rev.*, 1981, **39**, 181.
22. A. R. Gutierrez and A. W. Adamson, *J. Phys. Chem.*, 1978, **82**, 902.
23. M. Larsen, H. Macke, R. C. Rumfeldt and A. W. Adamson, *Inorg. Chim. Acta*, 1982, **57**, 229.
24. T. Ohno and S. Kato, *Bull. Chem. Soc. Jpn.*, 1973, **46**, 1602.
25. R. Bensasson, C. Salet and V. Balzani, *J. Am. Chem. Soc.*, 1976, **98**, 3722.
26. R. Fukuda. R. T. Walters, H. Macke and A. W. Adamson, *J. Phys. Chem.*, 1979, **83**, 2097.
27. A. W. Adamson, R. C. Fukuda and R. T. Walters, *J. Phys. Chem.*, 1981, **85**, 3206.
28. N. A. P. Kane-Maguire, C. G. Toney, B. Swiger, A. W. Adamson and R. E. Wright, *Inorg. Chim. Acta*, 1977, **22**, L11.
29. A. W. Adamson, *Discuss. Faraday Soc.*, 1960, **29**, 163.
30. K. Angermann, R. Schmidt, R. van Eldik, H. Kelm and F. Wasgestian, *Inorg. Chem.*, 1982, **21**, 1175.
31. F. Scandola, C. Bartocci and M. A. Scandola, *J. Am. Chem. Soc.*, 1973, **95**, 7988.
32. E. Zinato, P. Riccieri and A. W. Adamson, *J. Am. Chem. Soc.*, 1974, **96**, 375.
33. P. Riccieri and E. Zinato, *Inorg. Chem.*, 1980, **19**, 3279.
34. S. C. Pyke and R. G. Linck, *J. Am. Chem. Soc.*, 1971, **93**, 5281.
35. J. I. Zink, *J. Am. Chem. Soc.*, 1972, **94**, 8039.
36. M. Wrighton, H. B. Gray and G. S. Hammond, *Mol. Photochem.*, 1973, **5**, 165.
37. L. G. Vanquickenborne and A. Ceulemans, *J. Am. Chem. Soc.*, 1977, **99**, 2208; 1978, **100**, 475.
38. J. I. Zink, *Inorg. Chem.*, 1973, **12**, 1018.
39. L. G. Vanquickenborne and A. Ceulemans, *Inorg. Chem.*, 1978, **17**, 2730.
40. A. D. Kirk, *Coord. Chem. Rev.*, 1981, **39**, 225.
41. S. Behrendt, C. H. Langford and L. S. Frankel, *J. Am. Chem. Soc.*, 1969, **91**, 2236.
42. V. S. Sastri, R. W. Henwood, S. Behrendt and C.H. Langford, *J. Am. Chem. Soc.*, 1972, **94**, 753.
43. K. Angermann, R. van Eldik, H. Kelm and F. Wasgestian, *Inorg. Chem.*, 1981, **20**, 955.
44. K. Angermann, R. van Eldik, H. Kelm and F. Wasgestian, *Inorg. Chim. Acta*, 1981, **49**, 247.